doi:10.1093/plcell/koab266

THE PLANT CELL

THE PLANT CELL 2022: 34: 579–596

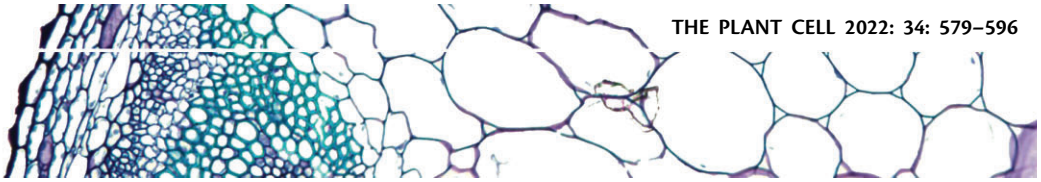

Research Article

Origin, loss, and regain of self-incompatibility in angiosperms

Hong Zhao ,[1,2] Yue Zhang ,[1,2] Hui Zhang ,[3] Yanzhai Song ,[1,2] Fei Zhao ,[2,4] Yu'e Zhang ,[1] Sihui Zhu ,[2,5] Hongkui Zhang ,[2,5] Zhendiao Zhou ,[2,5] Han Guo ,[1,2] Miaomiao Li ,[1,2] Junhui Li ,[1,2] Qiang Gao ,[1] Qianqian Han ,[1,2] Huaqiu Huang ,[1,2] Lucy Copsey ,[6] Qun Li ,[1] Hua Chen ,[2,5] Enrico Coen ,[6,*] Yijing Zhang [2,4,7,*] and Yongbiao Xue [1,2,5,8,*,†]

1 State Key Laboratory of Plant Cell and Chromosome Engineering, Institute of Genetics and Developmental Biology, and the Innovation Academy of Seed Design, Chinese Academy of Sciences, Beijing 100101, China
2 University of Chinese Academy of Sciences, Beijing 100049, China
3 College of Life Science, Northwest Normal University, Lanzhou 730070, China
4 National Key Laboratory of Plant Molecular Genetics, CAS Center for Excellence in Molecular Plant Sciences, Shanghai Institute of Plant Physiology and Ecology, Shanghai Institutes for Biological Sciences, Chinese Academy of Sciences, Shanghai 200032, China
5 Beijing Institute of Genomics, Chinese Academy of Sciences, and China National Centre for Bioinformation, Beijing 100101, China
6 John Innes Centre, Norwich NR47UH, UK
7 State Key Laboratory of Genetic Engineering, Collaborative Innovation Center of Genetics and Development, Department of Biochemistry, Institute of Plant Biology, School of Life Sciences, Fudan University, Shanghai 200438, China
8 Jiangsu Co-Innovation Center for Modern Production Technology of Grain Crops, Yangzhou University, Yangzhou 225009, China

*Author for correspondence: enrico.coen@jic.ac.uk; zhangyijing@fudan.edu.cn; ybxue@genetics.ac.cn
These authors contributed equally to this work (Ho.Z., Y.Z., Hu.Z., Y.S., F.Z., Y.Z., and S.Z.).
†Senior author.

Ho.Z. and Y.Z. performed the phylogenetic analyses of all the *S* genes and *S-like* genes. Y.Z. performed the functional analyses of *SLF*s of Rosaceae and Ranunculaceae. Hu.Z. and S.Z. performed the phylogenetic analyses of the *S* genes and *S-like* genes of type-1 SI. Y.S. performed the functional analyses of *AhSLF*s, *AmSLF*, and *AmFBX*. F.Z., Y.E.Z., Y.J.Z., and Q.G. performed genome analysis of *Antirrhinum hispanicum*. Ho.Z. and S.Z. performed ancestral state reconstruction analyses of SI systems, the genomic structure analyses of the linked Class I/II T2 *RNase*s and *FBA*/*FBK* loci of monocots and the related RNA-seq analyses, and H.K.Z assisted the RNA-seq analyses. Y.E.Z. and S.Z. performed transcriptional analyses of *A. hispanicum S-* and *S*-like-locus. Z.Z. and H.C. assisted the phylogenetic analyses of all the *S* genes and *S*-like genes. J.L. assisted the functional analysis of *SLF*s of Rosaceae. Ho.Z., H.H., and Q.L. assisted the functional analyses of *AhSLF*s. H.G. and M.L. performed functional analyses of *ShSLF*s. Q.H., L.C., and Y.E.Z prepared plant materials. Ho.Z., Y.Z., Hu.Z., F.Z., Z.Z., Q.G., H.C., E.C., Y.J.Z., and Y.X. analyzed data. E.C. conceived the idea of a high detoxification probability accounting for the origin of type-1 SI. Y.X. conceived the project and designed experiments. Ho.Z., Y.Z., E.C., and Y.X. wrote the manuscript with the input of all other authors.

The author responsible for distribution of materials integral to the findings presented in this article in accordance with the policy described in the Instructions for Authors (https://academic.oup.com/plcell) are: Yongbiao Xue (ybxue@genetics.ac.cn).

Abstract

The self-incompatibility (SI) system with the broadest taxonomic distribution in angiosperms is based on multiple *S-locus F-box* genes (*SLF*s) tightly linked to an *S-RNase* termed type-1. Multiple SLFs collaborate to detoxify nonself S-RNases while being unable to detoxify self S-RNases. However, it is unclear how such a system evolved, because in an ancestral system with a single SLF, many nonself S-RNases would not be detoxified, giving low cross-fertilization rates. In addition, how the system has been maintained in the face of whole-genome duplications (WGDs) or lost in other lineages remains unclear. Here we show that SLFs from a broad range of species can detoxify S-RNases from *Petunia* with a high detoxification probability, suggestive of an ancestral feature enabling cross-fertilization and subsequently modified as additional SLFs evolved.

Received July 13, 2021. Accepted October 26, 2021. Advance access publication November 4, 2021

IN A NUTSHELL

Background: Self-incompatibility (SI) is a widely occurring outcrossing mechanism leading to an inability of a fertile seed plant to produce zygotes after self-fertilization. Loss and regain of SI have frequently occurred during angiosperm evolution under the fluctuating selective pressures of inbreeding and outcrossing. Typically, among eudicots, there are four types of SI controlled by tightly linked female and male *S* genes forming the *S*-locus. For type-1 SI, the broadest taxonomically distributed SI system found in Plantaginaceae, Solanaceae, Rosaceae and Rutaceae, the *S*-locus contains *S-RNase* encoding the female *S* determinant, flanked by several *S-locus F-box* genes (*SLF*s) encoding the male *S* component. Multiple SLFs collaborate to detoxify non-self, but not self, S-RNases.

Question: We wanted to know how SI originated and evolved to be maintained or lost and the relationships among the four types of SI systems, by using a combination of genetic, phylogenomic and functional analyses.

Findings: First, the male *S* factor (SLFs) from a broad range of eudicots can detoxify S-RNases from *Petunia hybrida* with a high detoxification probability, suggesting that this is an ancestral system enabling outcrossing that was followed by the evolution of multiple *SLF*s. Many broad angiosperm species have likely established tightly linked female (T2 RNase) and male (F-Box Associated/F-Box Associated Kelch repeat) components to acquire type-1 SI. Third, loss of type-1 SI repeatedly occurred during angiosperm evolution to yield self-compatible lineages via *S*-locus deletion or duplication resulting from whole-genome duplications. However, other lineages regained SI either through deletion or inactivation of duplicate type-1 *S*-locus to maintain type-1 SI or evolved new SI of type-2, 3 or 4 systems.

Next steps: Our research reveals the highly dynamic evolutionary process of SI in angiosperms, providing a molecular evolutionary framework for SI studies. Further investigations into the function of type-1 *S*-locus from many angiosperm species will enrich our understanding of the origin and evolution of type-1 SI and shed light on the SI mechanisms of economic crops and grasses to enhance their breeding potentials.

We further show, based on its genomic signatures, that type-1 was likely maintained in many lineages, despite WGD, through deletion of duplicate *S*-loci. In other lineages, SI was lost either through *S*-locus deletions or by retaining duplications. Two deletion lineages regained SI through type-2 (Brassicaceae) or type-4 (Primulaceae), and one duplication lineage through type-3 (Papaveraceae) mechanisms. Thus, our results reveal a highly dynamic process behind the origin, maintenance, loss, and regain of SI.

Introduction

Self-incompatibility (SI), the inability of a fertile seed plant to produce a zygote after self-pollination, serves as a widely occurring outcrossing mechanism to prevent inbreeding in angiosperms. Approximately 40% of all angiosperm species possess SI. Various SI systems have evolved and are classified based on their associations with floral morphology (homo or heteromorphic SI; heterostyly), the genetic control of pollen SI phenotypes (sporophytic SI [SSI] or gametophytic SI [GSI]) or the number of *S*-loci (single to multiple) (de Nettancourt, 2001; Takayama and Isogai, 2005; Franklin-Tong, 2008; Zhang et al., 2009; Fujii et al., 2016). SI has been frequently lost and regained during evolution because of fluctuating selective pressures on selfing and outcrossing (de Nettancourt, 2001; Franklin-Tong, 2008). However, the mechanisms underlying origins and losses remain unclear. Here we address this problem through a combination of phylogenetic and functional tests across a broad range of taxa.

The system with the broadest taxonomic distribution, which we term type-1 SI, is gametophytic and based on linked pistil and pollen *S* components, corresponding to *S-RNase* and *S-locus F-box* (*SLF*), also named *S-haplotype-specific F-box* (*SFB*), respectively. So far, type-1 SI has been found in four eudicot families: Solanaceae, Plantaginaceae, Rosaceae, and Rutaceae, spanning two major clades (superrosids and superasterids; Anderson et al., 1986; McClure et al., 1989; Sassa et al., 1996; Xue et al., 1996; Lai et al., 2002; Ushijima et al., 2003; Sijacic et al., 2004; Qiao et al., 2004b; Sassa et al., 2007; Liang et al., 2020). In each case, an exemplar species (*Petunia inflata*, Spanish snapdragon [*Antirrhinum hispanicum*], wild cherry [*Prunus avium*], and pomelo [*Citrus maxima*]) has been shown to carry the *S*-locus containing an *S-RNase* flanked by a cluster of 9–37 *SLF* genes (Williams et al., 2014a; Kubo et al., 2015; Li et al., 2019; Liang et al., 2020). These genes function in SI, based on their specific expression in pistil and pollen, multiple alleles, correlation with *S* genotypes, mutations, and gene transformations that alter incompatibility or compatibility (Lee et al., 1994; Murfett et al., 1994; Royo et al., 1994; Sassa et al., 1997; Lai et al., 2002; Sijacic et al., 2004; Ushijima et al., 2004; Qiao et al., 2004b; Xue et al., 2009; Ye et al., 2018; Liang et al., 2020). Phylogenetic trees of T2 *RNase* genes have shown that *S-RNases* from species of both superrosids and superasterids cluster in a monophyletic group, suggesting a single origin of type-1 SI in the core eudicots (Xue et al., 1996; Igic and Kohn, 2001; Steinbachs and Holsinger, 2002; Vieira et al., 2008; Ramanauskas and Igic, 2017; Liang et al., 2020). Consistent with this idea, eight T2 RNases identified in monocots species such as rice (*Oryza sativa*) group into two

other classes of T2 RNases (Classes I and II) compared to S-RNases (Class III) (MacIntosh et al., 2010). However, a ribonuclease T2 family member (Aco001100) from pineapple (*Ananas comosus*) was shown to be tightly linked to several genes encoding F-box family members (Chen et al., 2019), indicating a likely presence of type-1 SI in monocots, although this remains to be confirmed through genetic linkage studies.

The type-1 SI system operates through multiple pollen-specific SLFs from one haplotype detoxifying pistil-specific S-RNases from other haplotypes, while not detoxifying S-RNases from its own haplotype (Sijacic et al., 2004; Qiao et al., 2004a, 2004b; Kubo et al., 2010; Liu et al., 2014; Zhao et al., 2021). Transgenic studies show that a single SLF can detoxify about 50% S-RNases from the same species (detoxification probability of 0.5), so multiple SLFs are needed within each haplotype to ensure high levels of cross-compatibility (Kubo et al., 2010; Williams et al., 2014b). However, it is unclear how such a system originated. If the ancestral *S*-locus contained a single *SLF* linked to an *S-RNase* (Sakai and Haluka, 2014; Sakai, 2016), a detoxification probability of 0.5 would lead to each haplotype only being able to pollinate 25% of females (assuming females are heterozygous and thus carry two S-RNases that need to be detoxified).

Type I SI system has been lost in multiple lineages (Fujii et al., 2016). Such losses may arise through several routes: (1) duplication of the *S*-locus to create two recombining haplotypes within the same genome, allowing SLFs from one haplotype to detoxify S-RNases from the other; (2) inactivation of the *S-RNase*; and (3) deletion of the entire *S*-locus. However, the relative contribution of these three mechanisms is not known. Moreover, it is unclear how type-1 SI was maintained in the face of whole-genome duplications (WGDs), which would have caused breakdown of SI via Route 1.

Depending on the loss mechanism, SI may have been regained through deletion of duplicate *S*-loci, reactivation of an *S-RNase*, or evolution of a new SI system. The latter process likely accounts for the other types of SI in eudicots (Fujii et al., 2016). Type-2 SI is the sporophytic Brassicaceae-type SI, controlled by a male *S*-locus cysteine-rich (SCR) protein/*S*-locus protein 11 and a female *S*-locus receptor kinase (SRK; Schopfer et al., 1999; Suzuki et al., 1999; Takasaki et al., 2000; Takayama et al., 2000). Type-3 is the gametophytic Papaveraceae-type SI, possessing the common poppy (*Papaver rhoeas*) stigma *S* (PrsS) and *P. rhoeas* pollen *S* (PrpS) (Foote et al., 1994; Wheeler et al., 2009). Type 4 is the sporophytic heterostyly of *Primula*, involving the *S*-locus supergene consisting of five genes encoding style length-determining cytochrome P450 (CYP), anther position-controlling GLOBOSA (GLO), a functionally unknown Conserved Cysteine Motif (CCM), Pumilio-like RNA-binding protein (PUM) and a Kelch repeat F-Box (KFB; Huu et al., 2016, 2020; Li et al., 2016). However, it is unclear what caused inactivation of the type-1 *S*-loci in these cases where SI was regained by a new mechanism.

Here we use a combination of phylogenetic and functional approaches to reveal a highly dynamic picture of SI evolution. We show that SLFs from a broad range of species can detoxify S-RNases from *Petunia* with a high detoxification probability, suggesting a likely mechanism for how type-1 SI might have originated. We further show, based on the distribution of type-1 *S*-locus signatures in the genome, that a type-1 SI system was maintained in many lineages, despite WGD, through deletion of duplicate *S*-loci. In other lineages, SI was lost either through deletion or duplications of the *S*-locus. Inactivation of the S-RNase was only detected in horticulturally selected lines, suggesting this route to self-compatibility (SC) is not favored in natural populations. Two deletion lineages regained SI through type-2 or type-4 mechanisms, while one duplication lineage regained SI through a type-3 mechanism.

Results

Phylogenetic analyses reveal that type-1 SI traces back to a single origin

Type-1 SI involves pistil S-RNases, which are members of the T2-type RNases. To elucidate the evolution of type-1 SI, we performed phylogenetic analyses of all T2 RNases from 12 species in four eudicot families (Plantaginaceae, Solanaceae, Rosaceae, and Rutaceae), two from monocot families (Poaceae and Bromeliaceae) and other angiosperms as well as gymnosperm species (Supplemental Data Set S1). Their T2 RNases fell into three clades: Classes I, II, and III. All S-RNases from the eudicot exemplar species were in Class III T2 RNase clade (Figure 1; Supplemental Figure S1). In addition to S-RNases, Class III T2 RNases of eudicot exemplar species included paralogs separate from the *S*-locus. For example, *Antirrhinum* contained a Class III T2 RNase on chromosome 7, whereas its *S*-locus maps to chromosome 8 (Li et al., 2019). These paralogs typically belonged to the same clade as *S-RNases* from the same plant family, suggesting that they arose through duplications within the family lineage. We refer to such paralogs as *S-like-RNases*.

To explore the evolution of the pollen component, we also performed phylogenetic analysis of SLF and other F-Box Associated/F-Box Associated Kelch (FBA/FBK) repeat proteins encoded by those genes linked to *S-like-RNases* in the eudicot exemplar species, or to Class I/II T2 *RNases* of monocot and other angiosperm species (Supplemental Data Set S2). The FBA/FBKs for the eudicot exemplar species all belonged to a single clade, which we refer to as the *SLF* subfamily, while those from monocots and other angiosperm species clustered into an outgroup (Figure 2; Supplemental Figure S2), thus supporting a single origin.

As with *S-RNases*, the *SLF* subfamily included paralogs outside the *S*-locus in exemplar species. These members typically belonged to the same clade as the *SLFs* from the same plant family, suggesting that they arose through duplications within the family lineage (Figure 2). We refer to such members as *S-like SLFs*. In exemplar species, they were always

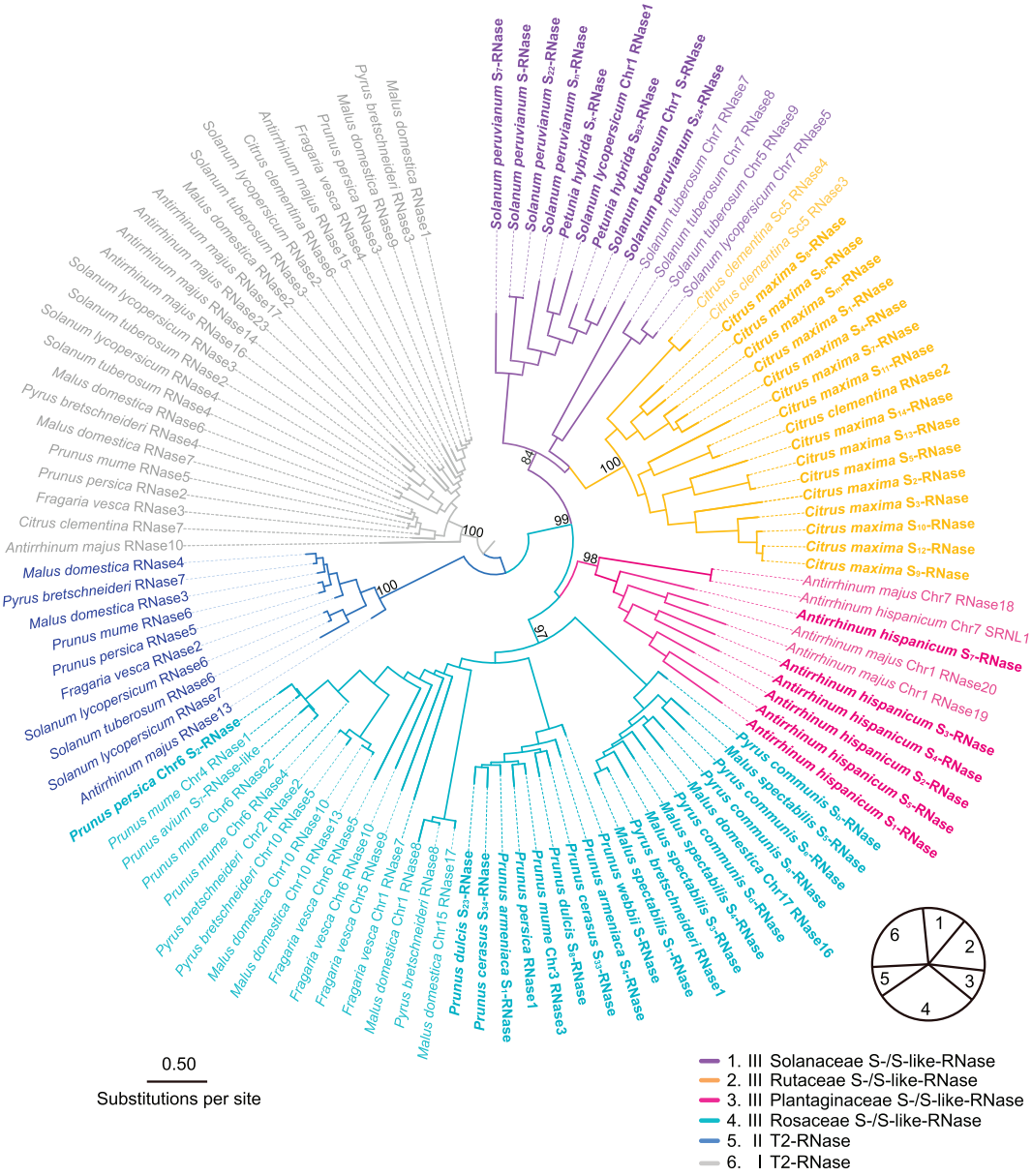

Figure 1 ML tree of the T2 RNase superfamily of the four exemplar families. ML phylogenetic tree of T2 RNases from 12 species of the four exemplar families with bootstrap confidence values >50%. I, II, and III indicate Class I, II, and III T2 RNases. Class III T2 RNases from different families and other types of T2 RNases are indicated by different branch colors. Bold fonts indicate functionally defined S-RNases. Chr, Chromosome; Sc, Scaffold. Please refer to Supplemental File S2 for the detailed bootstrap values.

closely linked to *S-like-RNases*. For example, *Antirrhinum* contained an *S-like SLF* (*AhChr7-SLFL1* and *AmChr7-SLFL1*) closely linked to an *S-like-RNase* on chromosome 7, suggesting duplication of an ancestral *S*-locus region (Li et al., 2019). However, in contrast to the *S*-locus, which contained multiple *SLFs*, the duplicated *S*-like locus on chromosome 7 contained only two *S-like SLFs*, one of which was a pseudogene (*AhChr7-ψSLF*) that was not expressed (Figure 3).

SLFs and *S-like SLFs* can detoxify *S-RNases* across superasterids

Expression of an *SLF* from a different *S*-haplotype in pollen will protect the pollen from its own encoded S-RNase, leading to breakdown of incompatibility, termed competitive interaction (Crane and Lewis, 1942; Lewis, 1947; Sijacic et al., 2004; Qiao et al., 2004b; Kubo et al., 2010; Zhao et al., 2021). These assays have largely been carried out using *SLFs* from the same species as the target *S-RNase*.

To examine the detoxification potential of *SLFs* and *S-like SLFs* across taxa, we introduced two *SLFs* from the S_5 locus of wild tomato (*Solanum habrochaites*) (ShS_5-*SLF5* or ShS_5-*SLF6*) (Supplemental Data Set S3) under the control of strong pollen promoters into the self-incompatible *Petunia hybrida* genotype S_3S_{3L} (PhS_3S_{3L}) (Supplemental Figure S3A). The transgenic plants ShS_5-*SLF5* PhS_3S_{3L} and ShS_5-*SLF6* PhS_3S_{3L} gained SC (Supplemental Figure S3B; Supplemental

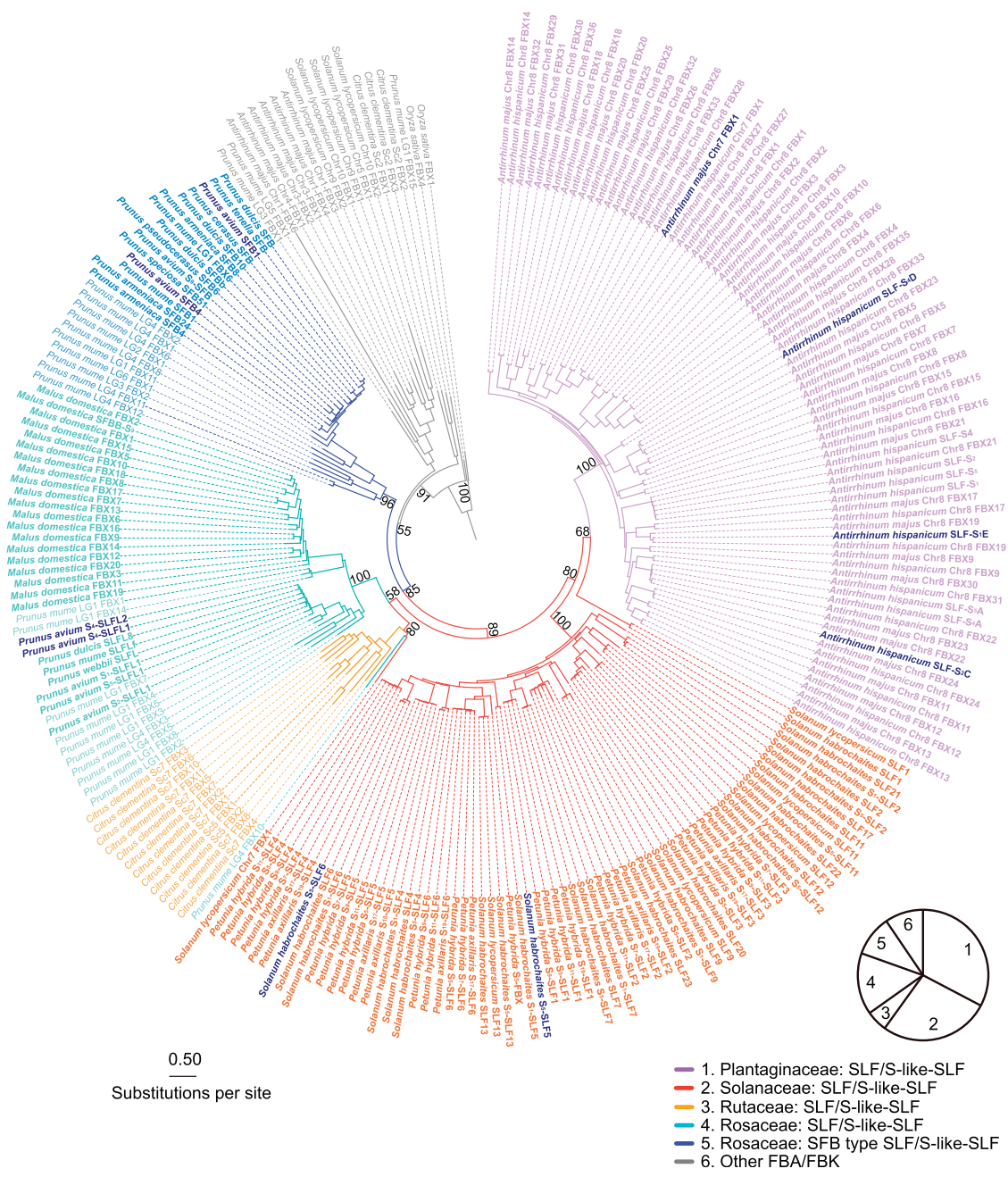

Figure 2 ML tree of FBA/FBKs of the four exemplar families. ML phylogenetic tree of FBAs/FBKs from 12 species of the four exemplar families with those from rice as a root and bootstrap confidence values > 50%. The SLFs from different families are indicated by different branch colors. Bold fonts indicate functionally defined SLFs. Green bold fonts indicate SLFs used for functional analysis. Please refer to Supplemental File S2 for the detailed bootstrap values.

Table 1). Self-progeny all carried transgenes, indicating that the observed SC results from competitive interaction (Supplemental Figure S3C). *S*-haplotype determinations showed that the transgenic line *Sh*S_5*-SLF5 Ph*S_3S_{3L} #2 produces 12 S_3S_{3L} and nine $S_{3L}S_{3L}$ progeny, but no S_3S_3 progeny. Similarly, the transgenic line *Sh*S_5*-SLF5 Ph*S_3S_{3L} #5 produced 14 S_3S_{3L} and nine $S_{3L}S_{3L}$ progeny, but no S_3S_3 progeny, indicating that ShS_5-SLF5 can inactivate the *P. hybrida* S_{3L}-RNase but not the S_3-RNase (Supplemental Table S1). The transgenic line *Sh*S_5*-SLF6 Ph*S_3S_{3L} #1 produced 11 S_3S_3 and 12 S_3S_{3L} progeny, and no $S_{3L}S_{3L}$ progeny, while the transgenic line *Sh*S_5*-SLF6 Ph*S_3S_{3L} #3 produced 13 S_3S_3 and 10 S_3S_{3L} progeny and no $S_{3L}S_{3L}$. Thus, ShS_5-SLF6 was able to inactivate the PhS_3-RNase but not the PhS_{3L}-RNase (Supplemental Table S1).

To examine the function of *SLF*s across a broader taxonomic distance, we introduced three *Antirrhinum SLF*s, one *S-like SLF* (Supplemental Data Set S3), and the FBA/FBK-encoding gene from *Antirrhinum majus Chr1-FBX6* (*AmChr1-FBX6*) that does not belong to the *SLF* subfamily,

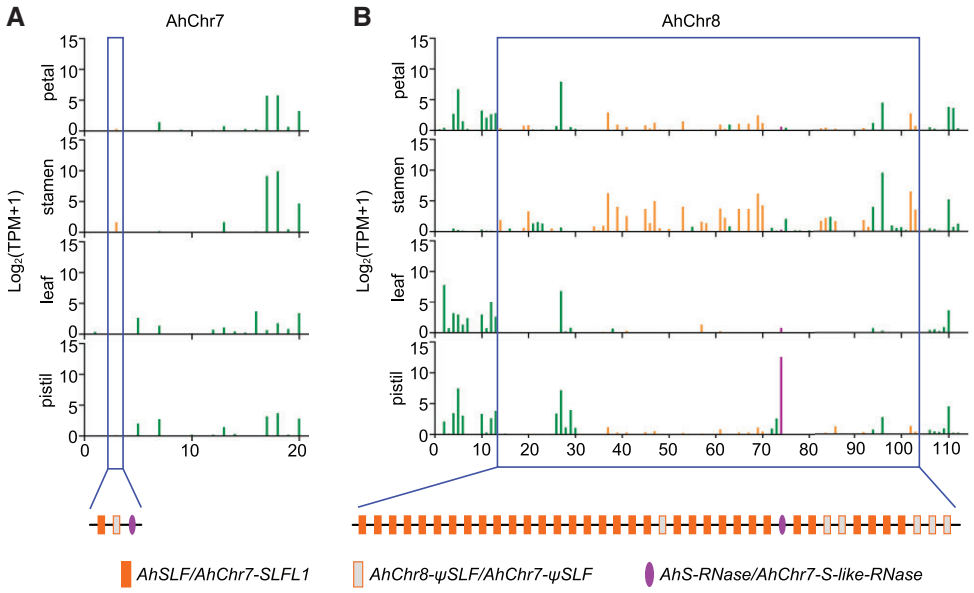

Figure 3 Transcriptional profiles of the type-1 *S*- and *S*-like-locus of *A. hispanicum*. The blue boxed regions denote the type-1 *S*-like-locus (A) and *S*-locus (B) covering 33 kb and 1.23 Mb, respectively. *x*-axes represent gene numbers. The expression levels of the *AhSLF* and *AhChr7-SLFL1* genes are shown in orange, *AhS-RNase*/*AhChr7-S-like-RNase* in violet and other unrelated genes in the region as green rectangles, for the indicated tissues on the *y*-axes. The violet ovals indicate the *AhS-RNase*/*AhChr7-S-like-RNase* and the rectangles the *AhSLFs*/*AhChr7-SLFL1* (orange) or *ψSLF* (light gray).

under the control of strong pollen promoters into the PhS_3S_{3L} background. Aniline blue staining showed that SI breaks down in transgenic plants expressing the *SLFs* and *S-like SLF* genes but not for the FBA/FBK-encoding gene (Supplemental Figure S4, A and B). Polymerase chain reaction (PCR) analysis showed that all self-progeny carry transgenes (Supplemental Figure S4C). For the transgenic lines carrying *Antirrhinum SLFs*, progeny testing showed that *Antirrhinum* SLFs can inactivate both PhS_{3L}- and PhS_3-RNase (Supplemental Table S2).

Expression of the *S-like SLF* (*AmChr7-SLFL1*) caused breakdown of SI by inactivating the PhS_{3L}-RNase (Supplemental Table S2). This result raised the question as to why the *S-like SLF* did not cause breakdown of SI in *A. hispanicum* by inactivating its S-RNase. Transcriptome analysis showed that *AhChr7-SLFL1* is expressed at a low level in the stamens of *A. hispanicum* compared to *AhChr7-ψSLF* and *S*-locus *SLFs*, 10–12 of which were expressed at high levels (Figure 3; Supplemental Data Sets S4 and S5). Thus, low expression of *AhChr7-SLFL1* may prevent it from causing breakdown of SI within *A. hispanicum*. In addition, the *S-like-RNase* was expressed at low levels in styles relative to the *S-RNase*, suggesting that it does not contribute to SI (Figure 3).

In summary, the ability to inactivate S-RNases is a feature of the *SLF* subfamily and acts across the Plantaginaceae and Solanaceae (superasterids).

SLFs and *S-like SLFs* can detoxify *S-RNases* across the Solanaceae and Rosaceae

The *S*-locus of *P. avium* (a member of the Rosaceae, representing superrosids) contains two types of *SLF* genes (*SLF* and *SFB* types) (Ushijima et al., 2003). Both types fall within the *SLF* family as described here (Figure 2). To test whether *SLFs* of *Prunus* can detoxify *S-RNases* in the Solanaceae, we introduced *PaSLFLs* (*SLF* type) and *PaSFBs* (*SFB* type) into the PhS_3S_{3L} background (Figure 4, A and B; Supplemental Data Set S3). PaS_4-*SLFL1* and PaS_4-*SLFL2* caused breakdown of SI of *P. hybrida* and progeny testing indicated that they can inhibit both PhS_{3L}-RNase and PhS_3-RNase (Figure 4, C and E; Supplemental Figure S5; Supplemental Table S3), *PaSFB1* and *PaSFB4* also inhibited both S-RNases (Figure 4, D and F; Supplemental Figure S5; Supplemental Table S3).

As a further test of detoxification range, we introduced an *SLF* from another member of the Rosaceae, apple (*Malus domestica*), into *P. hybrida*. Its *S*-locus only contains *SLF*-type *SLFs* named *S-locus F-box brothers* (*MdSFBBβ-S*$_9$) (Supplemental Data Set S3) and was able to detoxify both PhS_{3L}-RNase and PhS_3-RNase (Figure 5; Supplemental Table S3). Thus, both *SLFs* and *SFBs* of Rosaceae species can detoxify S-RNases in the superasterids.

SLFs and *S-like SLFs* from the Ranunculaceae can detoxify *S-RNases* in the Solanaceae

To further explore the detoxification range, we annotated homologs of *S-RNase* and *SLF* in Colorado blue columbine (*Aquilegia coerulea*) in the Ranunculaceae (Supplemental Figure S6). *Aquilegia coerulea* is cryptically self-incompatible because self-pollen produce fewer seeds than outcross pollen, likely due to inbreeding depression rather than SI (Montalvo, 1992). We detected four type-1 *S*-loci in this species. We introduced two *A. coerulea SLFs* (*AcSc4SLF4* and *AcSc4SLF5*) into the PhS_3S_{3L} background (Figure 6A; Supplemental Data

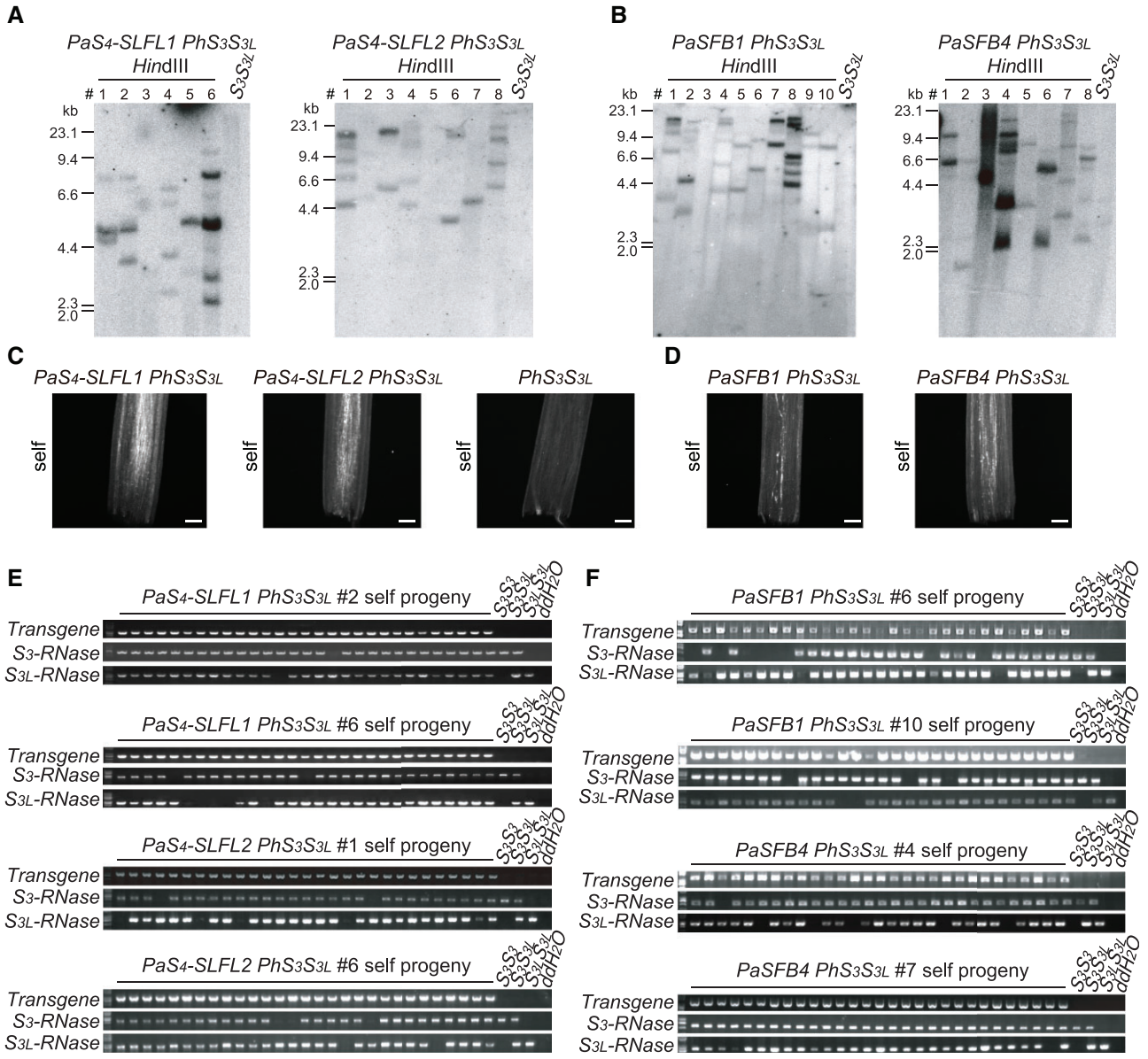

Figure 4 Both *SLF* and *SFB* type *SLF*s of *P. avium* function as pollen *S* factors. A and B, Southern blot analysis of T_0 transgenic lines harboring *PaS$_4$-SLFL1*, *PaS$_4$-SLFL2*, *PaSFB1*, and *PaSFB4*. C and D, Aniline blue staining of self-pollen tubes within the styles of *PaS$_4$-SLFL1 PhS$_3$S$_{3L}$*, *PaS$_4$-SLFL2 PhS$_3$S$_{3L}$*, the parental line *PhS$_3$S$_{3L}$*, *PaSFB1 PhS$_3$S$_{3L}$*, or *PaSFB4 PhS$_3$S$_{3L}$*. Pollen tubes are shown as dotted white lines. Scale bars, 200 μm. E and F, Transgene and *S*-haplotype determination by PCR analysis of self-progeny from transgenic plants of *PaS$_4$-SLFL1 PhS$_3$S$_{3L}$*, *PaS$_4$-SLFL2 PhS$_3$S$_{3L}$*, *PaSFB1 PhS$_3$S$_{3L}$*, and *PaSFB4 PhS$_3$S$_{3L}$*. Wild-type *PhS$_3$S$_{3L}$* was used as negative control for transgenes and as positive control for *PhS$_3$-RNase* and *PhS$_{3L}$-RNase*. *PhS$_3$S$_3$* and *PhS$_{3L}$S$_{3L}$* were used as positive or negative controls for corresponding *PhS-RNases*. ddH_2O was used as negative control for template DNA.

Set S3). Both *SLF*s caused breakdown of SI (Figure 6B) and progeny testing indicated that AcSC4-SLF4 can inhibit PhS$_3$-RNase, while AcSC4-SLF5 inhibited both PhS$_3$-RNase and PhS$_{3L}$-RNase (Figure 6C; Supplemental Table S4). The overall detoxification probability for all *SLF*s tested across taxa was 0.85, which was significantly higher than the probability of 0.186 within *Petunia* (Kubo et al., 2015) (assuming that the expected probability is 5/26 = 0.19, the observed probability is 22/26 = 0.85, χ^2 test (0.05) = 7.38, P = 0.0066).

A ribonuclease T2 family member (Aco001100) tightly linked to several F-box family member genes was identified in pineapple (*A. comosus*), indicating that it may have the potential to produce type-1 SI (Chen et al., 2019). Phylogenetic analysis indicated that this T2 RNase groups with Class I rather than Class III T2 RNases (Supplemental Figure S1). In addition to this locus, we identified another region (0.5 Mb) containing tightly linked Class I T2 *RNase* and two *FBK* genes on LG15. We also found three loci containing 1–3 Class I T2 *RNase* and 1–6 *FBK*/*FBA* genes on chromosomes 7–9 in the monocot species rice (Supplemental Figure S7). These genes were expressed constitutively in leaves, anthers (or

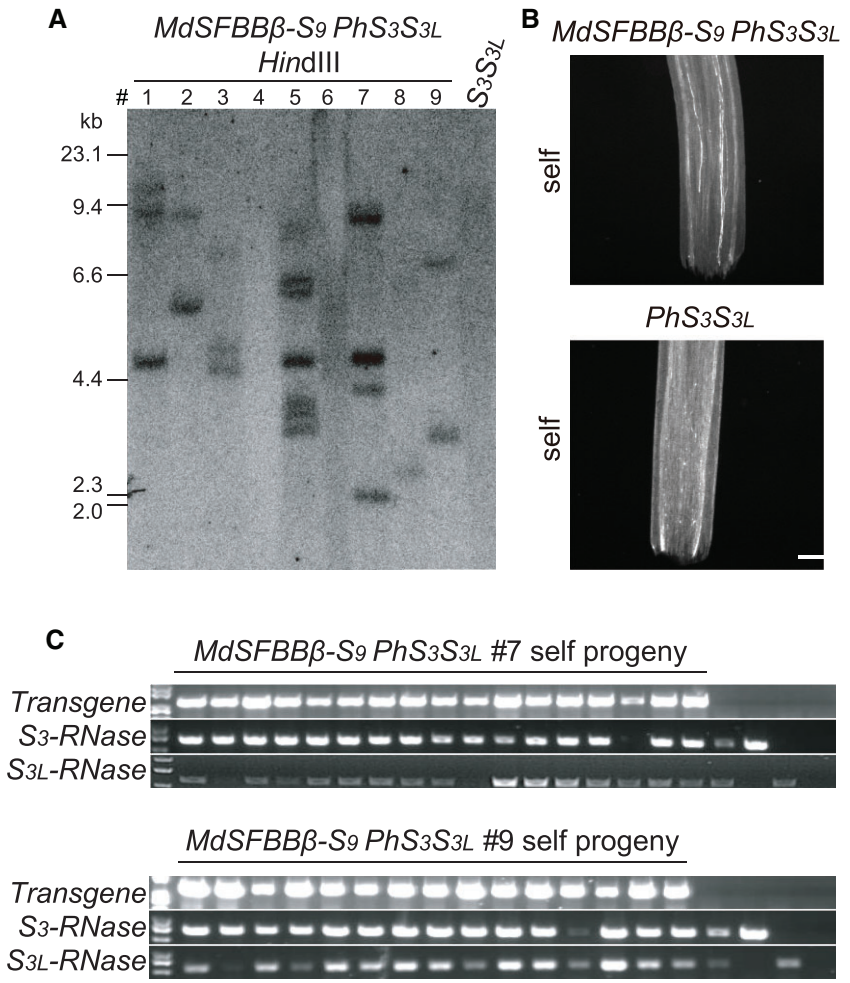

Figure 5 The *MdSFBBβ-S*$_9$ locus of *M. domestica* functions as the pollen *S* factor. A, Southern blot analysis of T_0 transgenic lines containing *MdSFBBβ-S*$_9$. B, Aniline blue staining of self-pollen tubes from *MdSFBBβ-S*$_9$ *PhS*$_3$*S*$_{3L}$ and *PhS*$_3$*S*$_{3L}$. Scale bars, 200 μm. C, Transgene and *S*-haplotype determination by PCR analysis of self-progeny from transgenic plants of *MdSFBBβ-S*$_9$ *PhS*$_3$*S*$_{3L}$. Positive and negative controls are identical to those in Figure 4E.

androecium) and pistils (or gynoecium) (Supplemental Figure S7), indicating a likely expression state of the ancestral type-1 *S*-locus. Pistil-specific (Class III T2/*S-RNase*) and pollen-specific (*SLFs*) expression may have evolved later to control eudicot type-1 SI. In the absence of genetic data, it is unclear whether the linked Class I T2 *RNase* and *FBK* genes found in monocots can confer type-1 SI. Ancestral state analysis showed that the common ancestor of angiosperms possessed linked Class I/II T2 *RNase*s and *FBA*/*FBK* genes. Whether the eudicot MRCA had linked Class I/II T2 *RNases*/*FBA*/*FBK* genes or whether a subfamily evolved toward Class III T2 *RNases*/*FBA*/*FBK* genes could not be determined with certainty (Figure 7; Supplemental Figure S8).

Loss and regain of SI

The early origin of type-1 *S*-locus/SI in eudicots and its ancestral states during the divergence of Nelumbonaceae, superasterids, and superrosids suggest that it has been repeatedly lost during evolution to give SC lineages (Figure 7; Supplemental Figure S8; Fujii et al., 2016). Loss of SI may arise through several routes: (1) Duplication of the *S*-locus to allow two haplotypes within the same genome, causing competitive interaction in the pollen; (2) Deletion or inactivation of components of the *S*-locus (e.g. *S-RNase*); or (3) Deletion of the entire *S*-locus (Figure 8A). Depending on the loss mechanism, SI may then have been regained in some SC lineages through: (1) inactivation or reduced expression of duplicate *S*-loci or *S* genes; (2) deletion of duplicates; (3) reactivation of the *S-RNase*; or (4) evolution of a new SI system (Figure 8A). To explore these possible scenarios, we annotated the complete type-1 *S*/*S*-like loci for 22 species representing 18 eudicot families on the basis of genome assembly quality (i.e. containing at least 1-Mb scaffolds, the smallest linkage region for type-1 *S*-/*S*-like loci) (Figure 8B; Supplemental Data Set S6). In addition, we classified type-1 *S*-loci into two types: active *S*-loci, which have putative functional *S-RNase* linked to functional *SLFs*, and inactive *S*-loci in which either the *S-RNase* or *SLF* appeared to be nonfunctional.

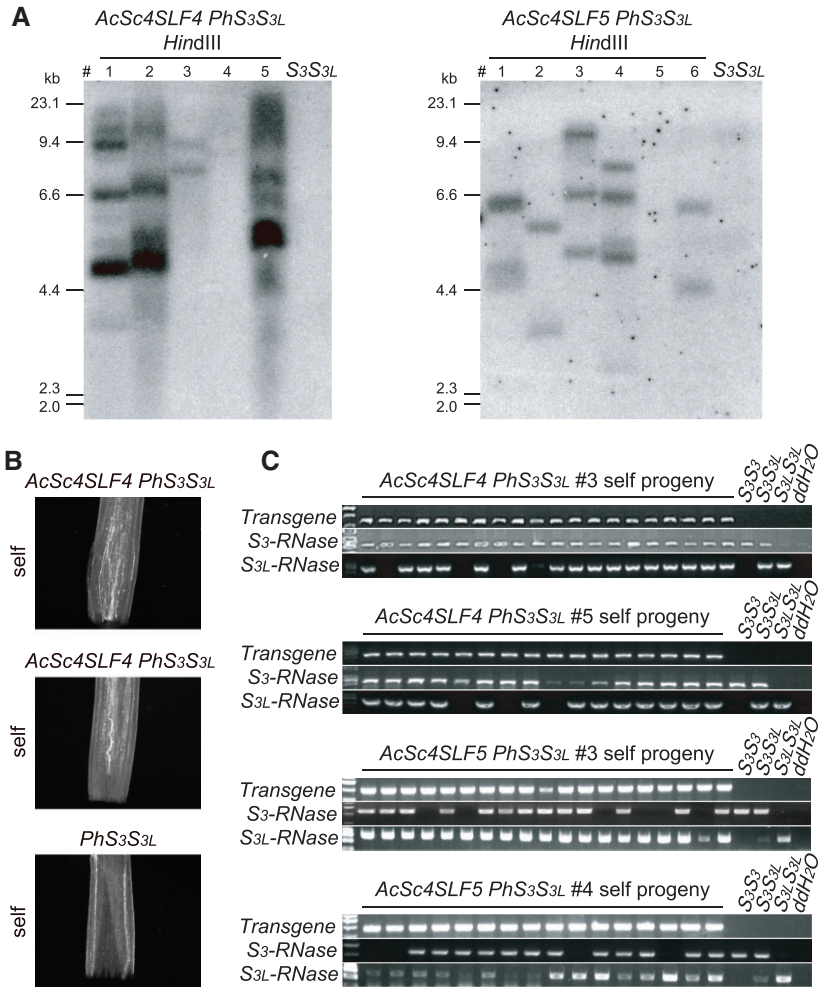

Figure 6 *S-like SLFs of A. coerulea function as the pollen S factors.* A, Southern blot analysis of T_0 transgenic lines containing *AcSc4SLF4* and *AcSc4SLF5*. B, Aniline blue staining of self-pollen tubes from *AcSc4SLF4* PhS_3S_{3L}, *AcSc4SLF5* PhS_3S_{3L}, and PhS_3S_{3L}. Scale bars, 200 μm. C, Transgene and S-haplotype determination by PCR analysis of self-progeny from transgenic plants of *AcSc4SLF4* PhS_3S_{3L} and *AcSc4SLF5* PhS_3S_{3L}. Positive and negative controls are identical to those in Figure 4E.

Based on the presence of linked T2-type *RNases* and *FBA/FBK* genes in both monocots and eudicots, their common ancestor likely had type-1 SI (Chen et al., 2019), and preceded the diversification of Classes I/II and III T2 *RNases*. Type-1 SI may have been subsequently lost in many monocots through Routes 1–3. In eudicot lineages, WGDs or triplications (WGT) would have led to duplications of the *S*-locus, causing loss of SI via Route 1 (Figure 8A), raising the question of how SI was maintained in those species that currently exhibit type-1 SI. *Antirrhinum hispanicum* contained a duplicate S-like locus that comprises a ψ*SLF*, an *SLF* expressed to low levels in stamens and an *S-like-RNase* expressed to low levels in styles (Figures 3 and 8, B), indicating that SI was regained via inactivation or reduced expression of duplicate copies (Route a) (Figure 8A). Chinese plum (*Prunus mume*) and clementine (*Citrus* × *clementina*) also had duplicate loci, one of which may have been degenerated in a similar manner. *Solanum habrochaites*, *C. maxima*, olive (*Olea europaea*), red date (*Ziziphus jujube*), and castor bean (*Ricinus communis*) had only one copy of the type-1 *S*-locus, indicating regain of SI via deletion of duplicates (Route b) (Figure 8, A and B).

Two SC species (*A. majus* and *S. lycopersicum*) showed either deletion (*A. majus*) or inactivation (*S. lycopersicum*; Tomato Genome Consortium, 2012) of the *S-RNase* (Route 2). Both species are horticultural varieties that have been selected for SC. Therefore, Route 2 for type-1 SI appears to have been favored in domestication but not in natural populations. Three other SC species, diploid cotton (*Gossypium raimondii*), common bean (*Phaseolus vulgaris*), and *A. coerulea* (Montalvo, 1992) had duplicate type-1 *S*-loci, indicating that SI was lost via Route 2 and not regained (Figure 8, A and B).

Origins of other types of SI in eudicots

We found no evidence of type-1 *S*-like-loci in species possessing type-2 (wild cabbage [*Brassica oleracea*]) or type-4 (cowslip [*Primula veris*]) SI (Figure 8B; Supplemental Data Set S6), suggesting ancestral loss of SI through deletion of

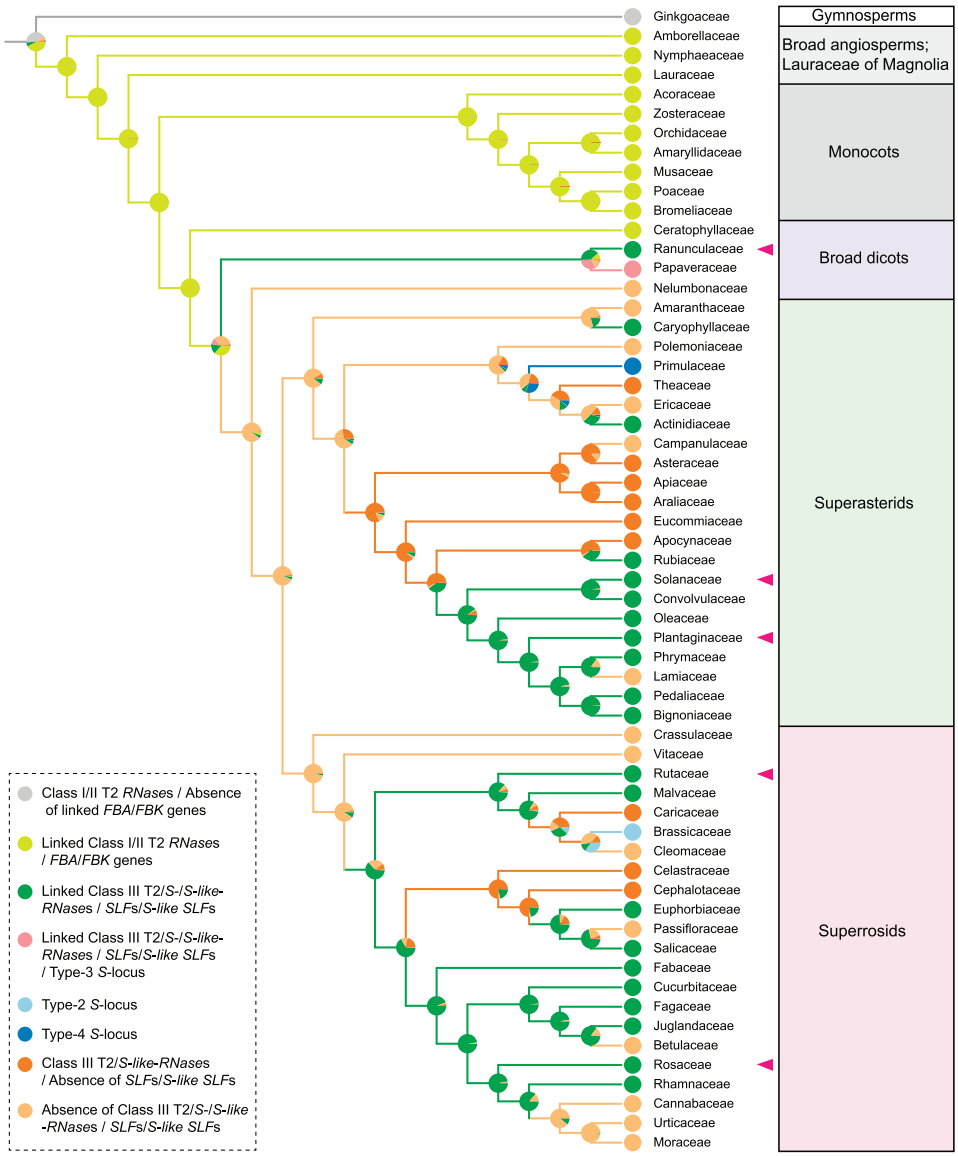

Figure 7 Evolution of the linked Class I/II/III T2 *RNases* and *FBA/FBK* genes inferred by PastML based on a family-level phylogenetic tree of the seed plants. Pie charts indicate probabilities of alternative ancestral states at nodes following analyses of eight traits shown as color-filled circles: possessing Class I/II T2 *RNases* with no linked *FBA/FBK* genes (light gray); possessing loci containing the linked Class I/II T2 *RNases* and *FBA/FBK* genes (light yellow-green); linked Class III T2/*S-/S-like-RNases* and *SLFs/S-like SLFs* (green); linked Class III T2/*S-/S-like-RNases* and *SLFs/S-like SLFs*/ type-3 *S*-locus (pink); type-2 *S*-locus (light blue); type-4 *S*-locus (blue); *S-like-RNases* with no linked *SLFs/S-like SLFs* (orange); and absence of both *S-/S-like-RNases* and *SLFs/S-like SLFs* (gold). Colors of the branches are consistent with those of the traits with the highest probabilities. Different evolutionary lineages are illustrated by different color ranges: white for gymnosperms (Ginkgoaceae), light gray for broad angiosperm families and Lauraceae of Magnolia, gray for monocots, purple for broad dicots, green for superasterids, and pink for superrosids. The magenta triangles indicate the five families with genetically demonstrated type-1 *S*-locus.

the type-1 *S*-locus (Route 3) and regain of SI through Route d (Figure 8A).

To examine the origin of type-2 SI, we annotated the pistil (*SRK*s) and pollen (*SCR*s) components in a total of 17 species from 15 genera of the Brassicaceae as well as in spider flower (*Cleome hassleriana*) of the Cleomaceae (Supplemental Figures S9 and S10; Supplemental Data Sets S7 and S8). We only detected *S*-loci, as defined by linkage between the pistil and pollen *S* genes, in the Brassicaceae (Supplemental Figure S9). Nevertheless, we detected *SCR-like* genes (expected threshold cut-off of 100) in upland cotton (*Gosssypium hirsutum*) and cacao (*Theobroma cacao*) of the Malvaceae and *S. pennellii* of the Solanaceae, but their linkage to *SRK-like* genes was absent (Supplemental Figures S9 and S10). Together with the ancestral state inference analyses of type-2 SI, these results indicated that its evolution occurred in the ancestor of the Brassicaceae (Figure 7). Arabidopsis had no detectable type-1 *S*-locus and its SC likely arose through inactivation of either *SRK* or *SCR* of the *S*-locus via Route

2, as reported previously (Kusaba et al., 2001; Tang et al., 2007; Tsuchimatsu et al., 2010; Figure 8).

To study the origin of type-4 SI, we analyzed the phylogenetic distribution of the S-locus supergene described in primrose (*Primula vulgaris*). The clustering of genes in the *S*-locus supergene was found in *P. vulgaris* of the Primulaceae but not in species from twelve other families representing monocots and eudicots, including neighboring families (Theaceae, Ericaceae, and Actinidiaceae). These findings suggested that the type-4 *S*-locus supergene evolved only in the Primulaceae (Figure 7; Supplemental Figure S11).

Opium poppy (*Papaver somniferum*), which exhibits type-3 SI, contained four type-1 *S*-like-loci, indicating ancestral loss of type-1 SI through duplication (Route 1) and subsequent regain of SI via Route d (Figure 8). To study the origin of type-3 SI, we analyzed the phylogenetic distribution *P. rhoeas PrsSs* and *PrpSs* (Supplemental Data Sets S9 and S10). Homologs of *PrsS* were widely detected in eudicots, but we only observed linkage with *PrpS* in the three *Papaveroideae* species examined (*P. rhoeas*, *P. somniferum*, and plume poppy [*Macleaya cordata*]), indicating that type-3 SI evolved in an ancestor of the *Papaveroideae* (Figure 7; Supplemental Figures S12 and S13).

Robusta coffee (*Coffea canephora*), which exhibits GSI, possessed two copies of type-1 *S*-loci, suggesting its regain of SI via either Route a or d (Figure 8). Similarly, common sunflower (*Helianthus annuus*), which exhibits SSI, had no type-1 *S*-like locus, indicating regain of SI via Route d (Figure 8).

Discussion

Evolution of type-1 SI must satisfy two constraints: (1) SLFs must not detoxify S-RNases from the same haplotype to maintain SI and (2) SLFs must be able to detoxify S-RNases from other haplotypes, allowing cross-compatibility. If the ancestral *S*-locus comprised a single *SLF* and *S-RNase* (Sakai and Haluka, 2014; Sakai, 2016), the first constraint might be readily satisfied by selection for an *S-RNase* that lies outside the detoxification range of the linked *SLF*. Satisfying the second constraint, however, depends on detoxification probability. If this probability is 0.5, as seen with *SLF*s from *Petunia*, pollen would be accepted by only 25% of nonself styles (Kubo et al., 2015). It is difficult to see how the SI system would have evolved with such a strong reproductive cost.

We found that SLFs from diverse taxa can detoxify *Petunia* S-RNases in 22 out of 26 cases, corresponding to a detoxification probability of 0.85. With such a probability, pollen would be accepted by 72% of styles for a single *SLF* linked to an *S-RNase* (Kubo et al., 2015), a much lower reproductive cost than for the probability of 0.5. Thus, we propose that the ancestral system involved SLFs with a high detoxification probability, as observed with our interspecific tests.

Once such a system was established, duplications of the *SLF* would further increase cross-compatibility. For example, pollen with two *SLF*s, each with 0.85 detoxification probability, would be accepted by 96% of styles compared to 72% with only one *SLF* (Kubo et al., 2015). Thus, selection would drive an increase in number of linked *SLF*s. However, there would also be selective pressure to narrow the target range to prevent detoxification within each haplotype (maintaining the first constraint of SI), which may act within each species to reduce target range over evolutionary time, resulting in the currently observed intraspecific detoxification probability of 0.5.

The linkage of *FBA*/*FBK* with T2 *RNase*s likely arose in the common ancestor of monocots and eudicots (Chen et al., 2019). We found that *SLF*s/*S-like SLF*s linked to Class III/*S-RNase*s existed exclusively in eudicots. Thus, if the common ancestor of eudicots and monocots had type-1 SI, this would have preceded the divergence between Classes I/II and III T2 *RNase*s.

Following the origin of type-1 SI, a pattern of losses and gains of SI may be inferred in eudicot lineages (Figure 8). Common routes to loss of SI are inactivation, deletion, or duplication of *S*-loci. Inactivation of the *S-RNase* alone is only observed in domesticated species, suggesting that there may be cost to this route in natural populations, perhaps because the *S-RNase* has a function outside SI. A *Prunus*-specific duplication of *F-box* genes has been proposed to generate a functional divergence between *SFB* and *SLFL*/*SFBB* leading to a distinct self-recognition SI system, in which SFB blocks self-S-RNase degradation (Morimoto et al., 2015; Akagi et al., 2016). In support of this self-recognition hypothesis, defective *SFB*s were found to be associated with SC in some *Prunus* species (Hauck et al., 2002; Ushijima et al., 2003, 2004; Tao and Iezzoni 2010). However, our finding that introducing *PaSFB* causes SC (i.e. promotes nonself-S-RNase ubiquitination and degradation) does not support the self-recognition hypothesis. A further observation supporting nonself-recognition rather than self-recognition is competitive interaction between two functional *S*-haplotypes of tetraploid Chinese sour cherry (*Prunus pseudocerasus* Lindl. CV. Nanjing Chuisi) leading to SC (Huang et al., 2008). More recently, the SC of *S4'* pollen containing defective *SFB* was shown to be mediated by S_4-*SLFL2* (Li et al., 2020). Thus, the validity of the self-recognition hypothesis for *Prunus* remains to be demonstrated.

Type-1 SI has been maintained in many species in the face of WGD through deletion or inactivation of duplicate copies of the *S*-locus. In two cases where type-1 *S*-loci were deleted, SI was regained by the evolution of new SI systems (types -2 and -4). In the case of type-3 SI, four type-1 *S*-like-loci were found in the genome, indicating loss of type-1 SI via duplication. For all SI types, we found that ancestral pistil (e.g. *S-RNase*, *SRK*, *PrsS*, and *CYP*) and pollen (e.g. *SLF*, *SCR*, *PrpS*, and *GLO*) factors, predate the formation of linked SI components. SI may therefore have evolved by duplications and rearrangements bringing the male and female components in tight linkage followed by neofunctionalization or

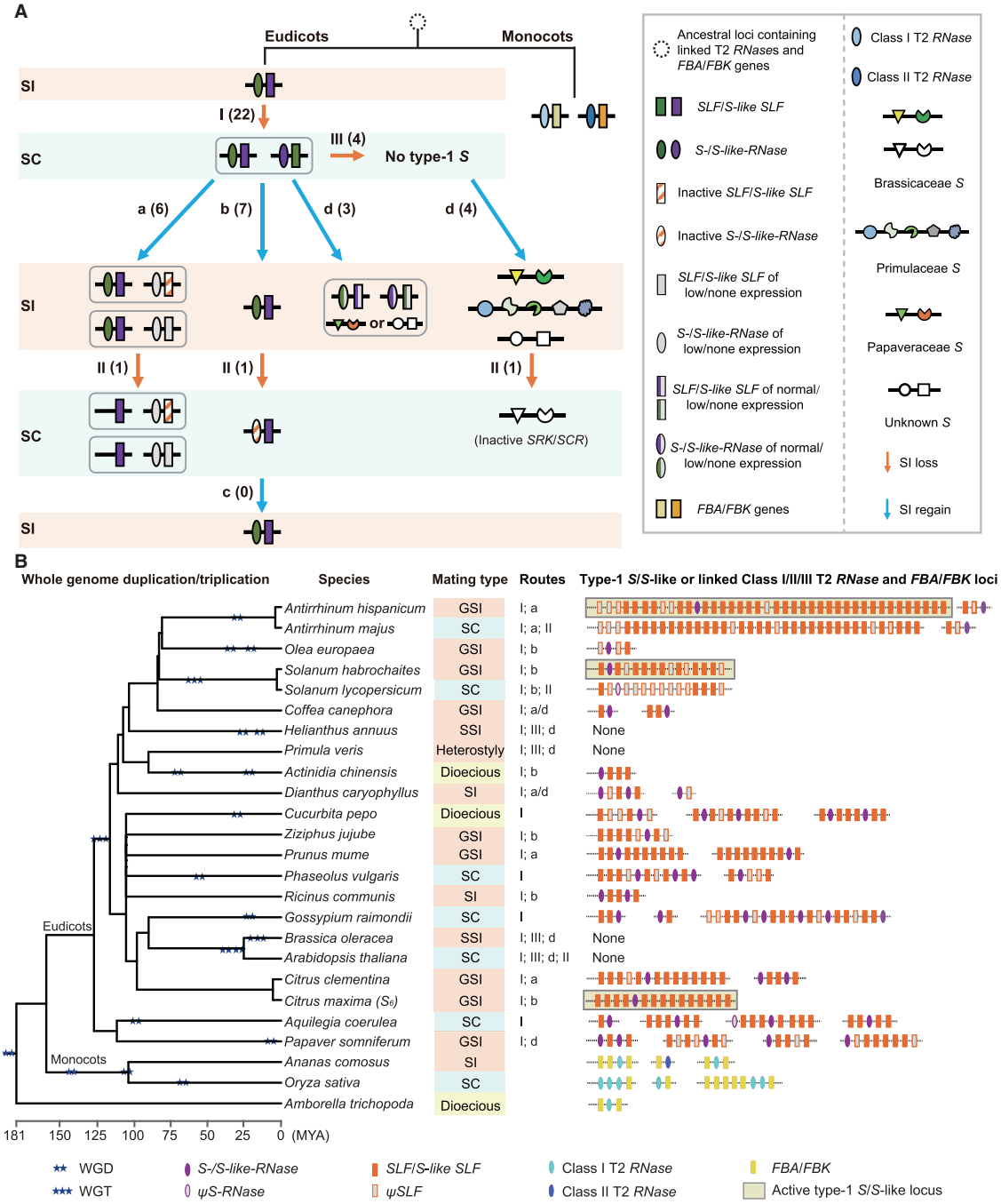

Figure 8 Routes of loss and regain of SI and their associations with type-1 *S*-/*S*-like loci in angiosperm species. A, Seven major routes contributing to the losses of SI leading to SC (I, II, and III) (orange arrow lines) and its regains (a–d) (blue arrow lines) in eudicots. The numbers in parentheses indicate the number of species that has taken each route among 22 eudicot species analyzed in this study. Color-filled rectangles and ovals represent *SLF*/*S-like SLF* and *S*-/*S-like-RNase* genes contributing to type-1 SI, respectively: green and violet for functional genes; light gray for low or no expression; orange stripe-filled for inactive genes. The same color (green or purple) relates to the corresponding *S*-/*S-like-RNase* and *SLF*/*S-like SLF* genes; for example, a green SLF is able to detoxify a green S-RNase. Gray rectangles with curved corners indicate that the *S*/*S*-like-loci are from the same genome. The *S*-loci (*S*) of type-2, -3, and -4 SI are denoted as Brassicaceae *S* (type-2) containing *SRK* and *SCR*, Papaveraceae *S* (type-3) *PrsS* and *PrpS* and Primulaceae *S* (type-4) *CYP*, *GLO*, *CCM*, *PUM*, and *KFB*, respectively. B, Genomic variations of type-1 *S*-/*S*-like loci and the loci of linked Class I/II T2 *RNases* and *FBA*/*FBK* genes in a total of 25 angiosperm species. Left: phylogenetic tree of eudicot species. Middle: orange, green, and yellow colored background represent GSI, SSI, late-acting SI or heterostyly, SC, and dioecious, respectively. Right: schematic diagrams of annotated genomic structures of linked Class I/II/III T2 *RNases* and *FBA*/*FBK* loci. Two and three stars depict WGD and WGT, respectively. Ovals filled with different colors indicate *S*-/*S-like-RNases* (violet), *ψS-RNases* (light gray), Class I (cyan) or II (blue) T2 *RNases* and rectangles *SLFs*/*S-like SLFs* (orange), *ψSLFs* (light gray), or *FBA*/*FBK* (yellow) and "None" indicates no type-1 *S*-/*S*-like-locus detected in these species. The numbers and letters labeled in the panel of "Routes" correspond to those indicated in (A).

subfunctionalization (Morimoto et al., 2015; Akagi et al., 2016).

Our results reveal a highly dynamic scenario for the evolution of SI. Initial establishment of an ancestral type-1 SI in angiosperms likely involved a single female (T2 *RNase*) and male (*FBK*/*FBA*) component coming into tight linkage. The ancestral single SLF had a high detoxification probability to allow type-1 SI to become established with sufficient cross-compatibility. Selection for further increase in cross-compatibility led to duplication and divergence of the *SLF* within the *S*-locus (Zhou et al., 2003; Kubo et al., 2015; Bod'ová et al., 2018; Li et al., 2019), while selection against detoxification of self-S-RNase led to reduced detoxification probabilities within species. This SI system was then maintained in many lineages despite WGD through deletion of duplicate *S*-loci. In other lineages SI was lost either through deletion or duplication of the *S*-locus. SI was then regained in some cases through novel male and female components coming together to create type-2–4 systems.

Materials and methods

Plant materials

Self-incompatible lines of *A. hispanicum* and *P. hybrida* were derived and maintained as previously described (Xue et al., 1996; Liu et al., 2014). *Solanum habrochaites* S_1S_5 (LA1777) was obtained from Tomato Genetic Resource Center (University of California, Davis) and *M. domestica* and *P. avium* from Dr Tianzhong Li's lab at China Agricultural University (CAU). The partial self-compatible line of *A. coerulea* was from Hongzhi Kong's lab at the Institute of Botany, the Chinese Academy of Sciences (CAS). All materials were planted in a greenhouse at the Institute of Genetics and Developmental Biology, CAS, except *M. domestica* and *P. avium*, which were planted in a CAU nursery.

Molecular techniques

Genomic DNA and total RNA were extracted as previously described (Lai et al., 2002; Liu et al., 2014). First-strand cDNAs were synthesized using SuperScript reverse transcriptase (Invitrogen, Carlsbad, MA, USA). The isolation of the coding sequences for *AhSLF*s, *PaSLFL*s, and *PaSFB*s were described previously (Zhou et al., 2003; Ikeda et al., 2004; Vaughan et al., 2006). The coding sequences for *ShSLF*s, *AcSLF*s, and *MdSFBB* were isolated from anther cDNAs of their source species. Restriction sites for BglII and SmaI were respectively introduced at the 5′- or 3′-end of *AhSLF*s and for XbaI and SacI at the 5′- or 3′-end of other *SLF*s. All *SLF*s coding sequences were ligated into modified pBI101 vectors as described previously (Qiao et al., 2004b; Liu et al., 2014) in which the tomato pollen-specific *LAT52* promoter was used to express *AhSLF*s; the PhS_3*A-SLF1* promoter was used for other *SLF*s. The accession numbers of *SLF*s and the primers used in this study are listed in Supplemental Data Sets S11 and S12, respectively.

Transformation of *P. hybrida*

The vectors containing *SLF*s were individually introduced into Agrobacterium (*Agrobacterium tumefaciens*) strain LBA4404 (Invitrogen, Carlsbad, CA, USA; http://www.thermofisher.com/) by electroporation and transformed into leaf disks of *P. hybrida* PhS_3S_{3L} as previously described (Lee et al., 1994; Qiao et al., 2004b). Southern blotting analysis was used to detect the transgenes. Briefly, genomic DNA (10 μg) was first digested with HindIII at 37°C for 4 h, then digested overnight after adding fresh HindIII. The DNA fragments were separated by electrophoresis overnight at 1 V/cm on a 0.8% (w/v) agarose gel and the separated fragments were transferred onto Hybond N + nylon membranes (Amersham, Buckinghamshire, UK, http://www.gelifesciences.com/). *Neomycin Phosphotransferase 2* (*NPTII*) probes were labeled with ^{32}P using the Prime-a-Gene labeling system (Promega, Madison, WI, USA; https://www.promega.com/). The pre-hybridization, hybridization and membrane washing steps were based on the operation manual (Russell and Sambrook, 2001). Radioactive signals were detected with a phosphor screen and a multifunctional laser scanning imager (GE Typhoon FLA9500).

Pollination analysis of transgenic plants

Self-pollination was performed using open flowers covered with paper bags before and after pollination to prevent cross pollination. Seedlings of one mature capsule from self-pollination for each transgenic line were used for genotyping. To examine the inheritance of *SLF* transgenes and the *S*-haplotypes of the progeny, PCRs with genomic DNA were performed using gene-specific primers listed in Supplemental Data Set S12. After amplification for 30 cycles, the products were separated by gel electrophoresis and detected by ethidium bromide staining.

Aniline blue staining of pollen tubes

About 48 h after self-pollination of transgenic plants and the wild-type PhS_3S_{3L}, the pollinated styles were fixed in ethanol: glacial acetic acid (3:1, v/v) solution for at least 8 h. Aniline blue staining of pollen tubes was then performed as described previously (Liu et al., 2014; Li et al., 2017) and the stained pollen tubes were observed under ultraviolet light by fluorescence microscopy.

Construction of family-/species-level phylogenetic trees and estimation of divergence times

Family-/species-level phylogenetic trees were constructed by phylomatic (version 3) (http://phylodiversity.net/phylomatic/) with the divergence times in those trees derived from TimeTree (http://www.timetree.org/) and WGD/WGTs from previous studies (Jiao et al., 2014; McKain et al., 2016; Leebens-Mack et al., 2019). Evolview (version 2) (http://www.evolgenius.info/evolview; He et al., 2016) and MEGAX (Sudhir et al., 2018) were used for visualization, annotation and management of the trees.

Annotations of the type-1 S-loci, type-1 S-like-loci and type-4 S-like-locus supergene

The genomic structures of the type-1 *S*-loci and type-1 *S*-like-loci were annotated based on the phylogenetic analyses of both Class III T2 *RNase*s and their linked *SLF*s/*S*-like *SLF*s, except for the *S*-locus of *A. majus* that was described previously (Li et al., 2019). *ψS-RNase*s and *ψSLF*s were annotated with in-frame stop codons. Based on the results of TBLASTN of the type-4 *S*-locus supergene, their homologs were searched within a 1-Mb window in the genomes of species other than Primulaceae with tandem repeats and reverse order allowed.

Phylogenetic analysis of the *S* and *S*-like genes

We obtained amino acid sequences corresponding to *S*-like genes by performing BLASTP or TBLASTN with BLAST version 2.2.29 against the protein or genome databases of the seed plants listed in Supplemental Data Set S13 using amino sequences of the proteins encoded by known *S* genes as queries. Databases were created (command: makeblastdb.exe -in filename.fasta -parse_seqids -hash_index -dbtype nucl/prot). BLAST was run using default settings with the expected threshold cut-off of 10^{-5} (homologous genes of *PUM*, *GLO*, *CYP*, *KFB* and *CCM*), 10^{-6} (T2 *RNase*s, *FBA*s/*FBK*s, and *PrsS*/*PrsS-like*s), 0.05 (*SCR*/*SCR-like*s and *PrpS*/*PrpS-like*s), and 0 (*SRK*/*SRK-like*s), respectively. In addition, BLAST for FBAs/FBKs was only performed in 33 species containing Class III T2 RNases except for *O. sativa*. Protein sequences obtained from BLAST were screened by InterProScan version 5.36 (Jones et al., 2014) (command: sh interproscan.sh -appl PfamA, TIGRFAM, SMART, SuperFamily, PRINTS -dp -f tsv, html –goterms –ipr lookup -t p -i filename.fa) and sequences containing a T2 RNase family or FBA1/FBA3 domain were retained. Then only *FBA*s/*FBK*s located near Class III T2 *RNase*s (upstream or downstream within 3 Mb) were obtained, except for species without such *FBA*s/*FBK*s. The full-length protein sequences of T2 RNases and FBAs/FBKs were aligned using L-INS-i method in MAFFT version 7.407 (Katoh and Standley, 2013) (command: nohup mafft –localpair –maxiterate 1000 –thread 64 $1 > "$NAME".afa &) and other proteins encoded by *S* genes using Muscle in MEGAX. We then manually curated the alignments using AliView (Larsson, 2014) or MEGAX to delete gaps and sequences without conserved motifs. To construct maximum likelihood (ML) trees, best-fitting amino acid substitution models were determined using ModelFinder within IQtree (-m MF -msub nuclear -nt AUTO) (Kalyaanamoorthy et al., 2017): a VT + R5 model for T2 RNase superfamily of the four exemplar families (Plantaginaceae, Solanaceae, Rutaceae, and Rosaceae), JTT + F + R7 for FBAs/FBKs of the four exemplar families, WAG + F + R4 for T2 RNases of *A. coerulea* and S-RNases of the four exemplar families, JTT + F + R5 for FBAs/FBKs of *A. coerulea* and SLFs of the four exemplar families, JTT + R4 for SRKs/SRK-likes, VT + R3 for SCRs/SCR-likes, VT + R6 for PrsSs/PrsS-likes, JTT + G4 for PrpSs/PrpS-likes, WAG + G for T2 RNases and VT + F + R10 for FBAs/FBKs. Then ML trees were inferred using IQ-TREE with default settings under the previously determined best-fitting amino acid substitution model. We measured branch support using the Ultrafast Bootstrap [UFBoot] algorithm with 1,000 replicates. MEGAX and iTOL (https://itol.embl.de/) was used for visualization, annotation and management of the trees.

Transcriptome analysis

Total RNA was extracted from four *A. hispanicum* tissues (leaf, pistil, stamen, and petal) using RNAprep Pure Plant Kit (Tiangen, Beijing, China). RNA purity and integrity were assessed using a NanoPhotometer® spectrophotometer (IMPLEN, CA, USA) and RNA Nano 6000 Assay Kit on a Bioanalyzer 2100 system (Agilent Technologies, Santa Clara, CA, USA), respectively. Sequencing libraries were generated using NEBNext UltraTM RNA Library Prep Kit for Illumina (NEB, USA). All libraries were sequenced using Illumina HiSeq 2000 (2 × 100 bp). Raw reads were quality-checked with FastQC96 (version 0.11.8) (http://www.bioinformatics.babraham.ac.uk/projects/fastqc; Andrews, 2010) and the resulting clean reads were aligned to the *A. hispanicum* genome (https://ngdc.cncb.ac.cn/gsa/browse, genome warehouse (GWH) accession GWHBFSA00000000, BioProject ID PRJCA006945) using STAR (version 2.7.1a) (Dobin et al., 2013) with parameters "-alignIntronMax 6000 -alignIntronMin 50" and the expression quantification for each gene was performed using RNA-seq by expectation maximization (RSEM) (Li and Dewey, 2011). The genome sequencing and assembly of *A. hispanicum* were performed as described by Li et al. (2019). The RNA-seq analyses of rice and pineapple T2 *RNase*s and *FBA*/*FBK* genes were performed based on the expression matrix data in Rice Genome Annotation Project and EBI-ENA under the accession number PRJEB33121 (Chen et al., 2019), respectively.

Ancestral state reconstruction

To evaluate the evolution of type-1 *S*-locus, five discrete traits were selected and codified as: possessing Class I/II T2 *RNase*s with no linked *FBA*/*FBK* genes; linked Class I/II T2 *RNase*s and *FBA*/*FBK* genes; linked Class III T2/*S*-/*S*-like-*RNase*s and *SLF*s/*S*-like *SLF*s; *S*-like-*RNase*s with no linked *SLF*s/*S*-like *SLF*s; and absence of both *S*-/*S*-like-*RNase*s and *SLF*s/*S*-like *SLF*s. Three additional traits (possession of type-2, type-3, or type-4 *S*-locus) were selected to reconstruct the evolution of these three types of *S*-loci as well as the evolutionary relationship of the four types of *S*-loci. Ancestral state reconstruction was conducted using PastML (https://pastml.pasteur.fr/help; Ishikawa et al., 2019) based on a family-level phylogenetic tree constructed as described above. ML method marginal posterior probabilities approximation under F81 model (Felsenstein, 1981) was used as recommended (Ishikawa et al., 2019) and iTOL (https://itol.embl.de/) was used for visualization and annotation of the results.

Calculation of probabilities for S-RNase detoxification by SLFs

To estimate the detoxification probability of n SLF types (P_n), we applied the equation "$P_n = 1 - (1 - P_R)^n$" reported in Kubo et al. (2015) assuming that S-RNase is independently recognized by each SLF with the same probability P_R. According to previous studies, a single SLF can recognize about 50% (i.e. $P_R = 0.5$) (Supplemental Data Set S3) or less (Kubo et al., 2015) S-RNases from the same species and the detoxification probability of pollen with a single SLF is 0.5 (i.e. P_n $(n = 1) = 0.5$) or less (Supplemental Data Set S3; Kubo et al., 2015). As SLFs from different species can detoxify *Petunia* S-RNases in 22/26 cases, the recognition probability is 0.85 (22/26) (i.e. $P_R = 0.85$) and pollen with a single SLF can detoxify 85% of S-RNases (i.e. P_n $(n = 1) = 0.85$) (Kubo et al., 2015), thus accepted by 72% (i.e. 0.85^2) of styles (assuming females are heterozygous and thus carrying two S-RNases to be detoxified). Likewise, pollen with two SLFs, each with 0.85 (P_R) recognition probability, would have a detoxification probability of 0.98 (i.e. P_n $(n = 2) = 0.98$) (Kubo et al., 2015) and would be accepted by 96% (i.e. 0.98^2) of females.

Accession numbers

All sequence data generated in the context of this manuscript have been deposited in the China National Center for Bioinformation Genome Sequence Archive database (https://ngdc.cncb.ac.cn/gsa/browse; Chen et al., 2021; CNCB-NGDC Members and Partners, 2021): Illumina reads for RNA-seq in the Genome Sequence Archive database (GSA accession CRA005238, BioProject ID PRJCA006940) and the whole-genome sequence data and assemblies of *A. hispanicum* in the Genome Warehouse database (GWH accession GWHBFSA00000000, BioProject ID PRJCA006945).

Supplemental data

The following materials are available in the online version of this article.

Supplemental Figure S1. ML tree of the T2 RNase superfamily of seed plants.

Supplemental Figure S2. ML tree of the FBA/FBKs of seed plants.

Supplemental Figure S3. *SLF*s of *S. habrochaites* function as pollen *S* factors.

Supplemental Figure S4. Both *SLF*s from the *S*-locus of *A. hispanicum* and an *SLFL* from an *S*-like-locus of *A. majus* function as the pollen *S* factors.

Supplemental Figure S5. Southern blot analysis of self-progeny plants of *PaS*$_4$*-SLFL1* PhS_3S_{3L}, *PaS*$_4$*-SLFL2* PhS_3S_{3L}, *PaSFB1* PhS_3S_{3L}, and *PaSFB4* PhS_3S_{3L}.

Supplemental Figure S6. Phylogenetic analyses of the *S* genes of *A. coerulea*.

Supplemental Figure S7. Transcript profiles of T2 *RNase*s and their linked *FBA*/*FBK* genes in *O. sativa* and *A. comosus*.

Supplemental Figure S8. Evolution of SI systems and their *S* genes in a family-level phylogenetic tree of the seed plants.

Supplemental Figure S9. The evolution of type-2 SI system in angiosperms.

Supplemental Figure S10. Phylogenetic analyses of the *S* genes of type-2 SI.

Supplemental Figure S11. The evolution of type-4 SI system in angiosperms.

Supplemental Figure S12. The evolution of type-3 SI system in angiosperms.

Supplemental Figure S13. Phylogenetic analyses of *S* genes of type-3 SI.

Supplemental Table S1. Pollination and genotype analyses of transgenic plants of *ShSLF*s PhS_3S_{3L}.

Supplemental Table S2. Pollination and genotype analyses of transgenic plants of *AhSLF*s PhS_3S_{3L} and *AmSLFL* PhS_3S_{3L}.

Supplemental Table S3. Pollination and genotype analyses of transgenic plants of *PaSLFL*s PhS_3S_{3L}, *PaSFB*s PhS_3S_{3L}, and *MdSFBB* PhS_3S_{3L}.

Supplemental Table S4. Pollination and genotype analyses of transgenic plants of *AcSLF*s PhS_3S_{3L}.

Supplemental Data Set S1. Accession numbers of T2 *RNase* genes used in this study.

Supplemental Data Set S2. Accession numbers of *FBX*/*FBA*/*FBK* genes used in this study.

Supplemental Data Set S3. Summary of species, *SLF*s/*SLFL*s/*SFB*s used for transformation, and *S* haplotypes of compatible transgenic pollen caused by competitive interaction.

Supplemental Data Set S4. RNA-seq data of the *S*-locus in four tissues of *A. hispanicum* used in this study.

Supplemental Data Set S5. RNA-seq data of the *S*-like-locus in four tissues of *A. hispanicum* used in this study.

Supplemental Data Set S6. Species annotated with linked pistil-pollen gene pairs in this study.

Supplemental Data Set S7. Accession numbers of *SRK*/*SRKL*, genes used in this study.

Supplemental Data Set S8. Accession numbers of *SCR*/annotated *SCR* genes used in this study.

Supplemental Data Set S9. Accession numbers of *PrsS*/annotated *PrsS* genes used in this study.

Supplemental Data Set S10. Accession numbers of *PrpS*/annotated *PrpS* genes used in this study.

Supplemental Data Set S11. Accession numbers of transgenic *FBX*/*SLF* genes used in this study.

Supplemental Data Set S12. Primer list.

Supplemental Data Set S13. Genome databases used in this study.

Supplemental File S1. Fasta files of the sequence alignments corresponding to the phylogenetic analyses of the type-1–4 *S* genes.

Supplemental File S2. Tree text files corresponding to the phylogenetic analyses in Figures 1, 2, 7, and 8 and Supplemental Figures S1, S2, S6, and S8–S13.

Acknowledgments

We thank Dr Hongzhi Kong of Institute of Botany of CAS for providing *A. coerulea* and Dr Desmond Bradley for critically reading of the manuscript.

Funding

This work was supported by the National Natural Science Foundation of China (32030007) and the Strategic Priority Research Program of the CAS (XDB27010302 and XDA26030302).

Conflict of interest statement. The authors declare that they have no conflict of interest.

References

Anderson MA, Cornish EC, Mau SL, Williams EG, Hoggart R, Atkinson A, Bonig I, Grego B, Simpson R, Roche PJ, et al. (1986) Cloning of cDNA for a stylar glycoprotein associated with expression of self-incompatibility in *Nicotiana alata*. Nature **321**: 38–44

Andrews S (2010) FastQC: A Quality Control Tool for High Throughput Sequence Data. v.0.11.8, Brabham Bioinformatics, Brabham Institute, Babraham, Cambridgeshire

Akagi T, Henry IM, Morimoto T, Tao R (2016) Insights into the Prunus-specific S-RNase-based self-incompatibility system from a genome-wide analysis of the evolutionary radiation of *S* locus-related F-box genes. Plant Cell Physiol **57**: 1281–1294

Bod'ová K, Priklopil T, Field DL, Barton NH, Pickup M (2018) Evolutionary pathways for the generation of new self-incompatibility haplotypes in a nonself-recognition system. Genetics **209**: 861–883

Chen LY, VanBuren R, Paris M, Zhou H, Zhang X, Wai CM, Yan H, Chen S, Alonge M, Ramakrishnan S, et al. (2019) The bracteatus pineapple genome and domestication of clonally propagated crops. Nat Genet **51**: 1549–1558

Chen M, Ma Y, Wu S, Zheng X, Kang H, Sang J, Xu X, Hao L, Li Z, Gong Z, et al. (2021) Genome Warehouse: a public repository housing genome-scale data. Genom Proteom Bioinform doi: 10.1016/j.gpb.2021.04.001

CNCB-NGDC Members and Partners (2021) Database resources of the national genomics data center, China national center for bioinformation in 2021. Nucleic Acids Res **49**: D18–D28

Crane MB, Lewis D (1942) Genetical studies in pears. III. Incompatibility and sterility. J Genet **43**: 31–42

Dobin A, Davis CA, Schlesinger F, Drenkow J, Zaleski C, Jha S, Batut P, Chaisson M, Gingeras TR (2013) STAR: ultrafast universal RNA-seq aligner. Bioinformatics **29**: 15–21

Felsenstein J (1981) Evolutionary trees from DNA sequences: a maximum likelihood approach. J Mol Evol **17**: 368–376

Foote HC, Ride JP, Franklin-Tong VE, Walker EA, Lawrence MJ, Franklin FC (1994) Cloning and expression of a distinctive class of self-incompatibility (*S*) gene from *Papaver rhoeas* L. Proc Natl Acad Sci USA **91**: 2265–2269

Franklin-Tong VE (2008) Self-incompatibility in Flowering Plants, Springer, Berlin Heidelberg, Germany

Fujii S, Kubo K, Takayama S (2016) Non-self- and self-recognition models in plant self-incompatibility. Nat Plants **2**: 16130

Hauck NR, Yamane H, Tao R, Iezzoni AF (2002) Self-compatibility and incompatibility in tetraploid sour cherry (Prunus cerasus L.). Sex Plant Reprod **15**: 39–46

Huang SX, Wu HQ, Li YR, Wu J, Zhang SJ, Heng W, Zhang SL (2008) Competitive interaction between two functional *S*-haplotypes confer self-compatibility on tetraploid Chinese cherry (*Prunus pseudocerasus* Lindl. CV. Nanjing Chuisi). Plant Cell Rep **27**: 1075–1085

He Z, Zhang H, Gao S, Lercher MJ, Chen WH, Hu S (2016) Evolview v2: an online visualization and management tool for customized and annotated phylogenetic trees. Nucleic Acids Res **44**: W236–W241

Huu CN, Kappel C, Keller B, Sicard A, Takebayashi Y, Breuninger H, Nowak MD, Baurle I, Himmelbach A, Burkart M, et al. (2016) Presence versus absence of CYP734A50 underlies the style-length dimorphism in primroses. Elife **5**: e17956

Huu CN, Keller B, Conti E, Kappel C, Lenhard M (2020) Supergene evolution via stepwise duplications and neofunctionalization of a floral-organ identity gene. Proc Natl Acad Sci USA **117**: 23148–23157

Igic B, Kohn JR (2001) Evolutionary relationships among self-incompatibility RNases. Proc Natl Acad Sci USA **98**: 13167–13171

Ikeda K, Igic B, Ushijima K, Yamane H, Hauck NR, Nakano R, Sassa H, Iezzoni AF, Kohn JR, Tao R (2004) Primary structural features of the *S* haplotype-specific F-box protein, SFB, in *Prunus*. Sex Plant Reprod **16**: 235–243

Ishikawa SA, Zhukova A, Iwasaki W, Gascuel O (2019) A fast likelihood method to reconstruct and visualize ancestral scenarios. Mol Biol Evol **36**: 2069–2085

Jiao Y, Li J, Tang H, Paterson AH (2014) Integrated syntenic and phylogenomic analyses reveal an ancient genome duplication in monocots. Plant Cell **26**: 2792–2802

Jones P, Binns D, Chang HY, Fraser M, Li W, McAnulla C, McWilliam H, Maslen J, Mitchell A, Nuka G, et al. (2014) InterProScan 5: genome-scale protein function classification. Bioinformatics **30**: 1236–1240

Kalyaanamoorthy S, Minh BQ, Wong TK, Von Haeseler A, Jermiin LS (2017) ModelFinder: fast model selection for accurate phylogenetic estimates. Nat Methods **14**: 587–589

Katoh K, Standley DM (2013) MAFFT multiple sequence alignment software version 7: improvements in performance and usability. Mol Biol Evol **30**: 772–780

Kubo K, Entani T, Takara A, Wang N, Fields AM, Hua Z, Toyoda M, Kawashima S, Ando T, Isogai A, et al. (2010) Collaborative non-self recognition system in S-RNase-based self-incompatibility. Science **330**: 796–799

Kubo K, Paape T, Hatakeyama M, Entani T, Takara A, Kajihara K, Tsukahara M, Shimizu-Inatsugi R, Shimizu KK, Takayama S (2015) Gene duplication and genetic exchange drive the evolution of S-RNase-based self-incompatibility in *Petunia*. Nat Plants **1**: 14005

Kusaba M, Dwyer K, Hendershot J, Vrebalov J, Nasrallah JB, Nasrallah ME (2001) SI in the genus Arabidopsis: characterization of the *S* locus in the outcrossing *A. lyrata* and its autogamous relative *A. thaliana*. Plant Cell **13**: 627–643

Lai Z, Ma W, Han B, Liang L, Zhang Y, Hong G, Xue Y (2002) An F-box gene linked to the self-incompatibility (*S*) locus of *Antirrhinum* is expressed specifically in pollen and tapetum. Plant Mol Biol **50**: 29–42

Larsson A (2014) AliView: a fast and lightweight alignment viewer and editor for large datasets. Bioinformatics **30**: 3276–3278

Lee HS, Huang S, Kao TH (1994) *S* proteins control rejection of incompatible pollen in *Petunia inflata*. Nature **367**: 560–563

Leebens-Mack JH, Carpenter EJ, Deyholos MK, Gitzendanner MA, Graham SW, Grosse I, Li Z, Melkonian M, Mirarab S, Porsch M, et al. (2019) One thousand plant transcriptomes and the phylogenomics of green plants. Nature**574** 679–685

Lewis D (1947) Competition and dominance of incompatibility alleles in diploid pollen. Heredity **1**: 85–108

Li B, Dewey CN (2011) RSEM: accurate transcript quantification from RNA-Seq data with or without a reference genome. BMC Bioinformatics **12**: 323

Li J, Cocker JM, Wright J, Webster MA, McMullan M, Dyer S, Swarbreck D, Caccamo M, Oosterhout CV, Gilmartin PM (2016) Genetic architecture and evolution of the *S* locus supergene in *Primula vulgaris*. Nat Plants **2**: 16188

Li J, Zhang Y, Song Y, Zhang H, Fan J, Li Q, Zhang D, Xue Y (2017) Electrostatic potentials of the S-locus F-box proteins contribute to the pollen *S* specificity in self-incompatibility in *Petunia hybrida*. Plant J **89**: 45–57

Li M, Zhang D, Gao Q, Luo Y, Zhang H, Ma B, Chen C, Whibley A, Zhang Y, Cao Y, et al. (2019) Genome structure and evolution of *Antirrhinum majus* L. Nat Plants **5**: 174–183

Li Y, Duan X, Wu C, Yu J, Li W (2020) Ubiquitination of S_4-RNase by S-LOCUS F-BOX LIKE2 contributes to self-compatibility of Sweet Cherry 'Lapins'. Plant Physiol **184**: 1702–1716

Liang M, Cao Z, Zhu A, Liu Y, Tao M, Yang H, Xu Q, Jr, Wang S, Liu J, Li Y, et al. (2020) Evolution of self-compatibility by a mutant *Sm-RNase* in *Citrus*. Nat Plants **6**: 131–142

Liu W, Fan J, Li J, Song Y, Li Q, Zhang Y, Xue Y (2014) SCF^{SLF}-mediated cytosolic degradation of S-RNase is required for cross-pollen compatibility in S-RNase-based self-incompatibility in *Petunia hybrida*. Front Genet **5**: 228

MacIntosh GC, Hillwig MS, Meyer A, Flagel L (2010) RNase T2 genes from rice and the evolution of secretory ribonucleases in plants. Mol Genet Genomics **283**: 381–396

McClure BA, Haring V, Ebert PR, Anderson MA, Simpson RJ, Sakiyama F, Clarke AE (1989) Style self-incompatibility gene products of *Nicotiana alata* are ribonucleases. Nature **342**: 955–957

McKain MR, Tang H, McNeal JR, Ayyampalayam S, Davis JI, dePamphilis CW, Givnish TJ, Pires JC, Stevenson DW, Leebens-Mack JH (2016) A phylogenomic assessment of ancient polyploidy and genome evolution across the poales. Genome Biol Evol **8**: evw060

Montalvo AM (1992) Relative success of self and outcross pollen comparing mixed- and single-donor pollinations in *Aquilegia caerulea*. Evolution **46**: 1181–1198

Murfett J, Atherton TL, Mou B, Gasser CS, McClure BA (1994) S-RNase expressed in transgenic *Nicotiana* causes *S*-allele-specific pollen rejection. Nature **367**: 563–566

Morimoto T, Akagi T, Tao R (2015) Evolutionary analysis of genes for S-RNase-based self-incompatibility reveals *S* locus duplications in the ancestral Rosaceae. Hort J **84**: 233–242

de Nettancourt D (2001) Incompatibility and Incongruity in Wild and Cultivated Plants. Springer, Berlin Heidelberg, Germany

Qiao H, Wang H, Zhao L, Zhou J, Huang J, Zhang Y, Xue Y (2004a) The F-box protein AhSLF-S2 physically interacts with S-RNases that may be inhibited by the ubiquitin/26S proteasome pathway of protein degradation during compatible pollination in *Antirrhinum*. Plant Cell **16**: 582–595

Qiao H, Wang F, Zhao L, Zhou J, Lai Z, Zhang Y, Robbins TP, Xue Y (2004b) The F-box protein AhSLF-S2 controls the pollen function of S-RNase-based self-incompatibility. Plant Cell **16**: 2307–2322

Ramanauskas K, Igic B (2017) The evolutionary history of plant T2/S-type ribonucleases. Peer J **5**: e3790

Royo J, Kunz C, Kowyama Y, Anderson M, Clarke AE, Newbigin E (1994) Loss of a histidine residue at the active site of *S*-locus ribonuclease is associated with self-compatibility in *Lycopersicon peruvianum*. Proc Natl Acad Sci USA **91**: 6511–6514

Russell DW, Sambrook J (2001) Molecular Cloning: A Laboratory Manual. Cold Spring Harbor Laboratary Press, Cold Spring Harbor, NY

Sakai S. (2016) How have self-incompatibility haplotypes diversified? Generation of new haplotypes during the evolution of self-incompatibility from self-compatibility. Am Nat **188**: 163–174

Sakai S, Haluka W (2014) Initial invasion of gametophytic self-incompatibility alleles in the absence of tight linkage between pollen and pistil *S* alleles. Am Nat **184**: 248–257

Sassa H, Koba T, Ikehashi H, Nishio T, Kowyama Y, Hirano H (1996) Self-incompatibility (*S*) alleles of the Rosaceae encode members of a distinct class of the T2/S ribonuclease superfamily. Mol Gen Genet **250**: 547–557

Sassa H, Hirano H, Nishio T, Koba T (1997) Style-specific self-compatible mutation caused by deletion of the *S-RNase* gene in Japanese pear (*Pyrus serotina*). Plant J **12**: 223–227

Sassa H, Kakui H, Miyamoto M, Suzuki Y, Hanada T, Ushijima K, Kusaba M, Hirano H, Koba T (2007) *S* locus F-box brothers: multiple and pollen-specific F-box genes with *S* haplotype-specific polymorphisms in apple and Japanese pear. Genetics **175**: 1869–1881

Schopfer CR, Nasrallah ME, Nasrallah JB (1999) The male determinant of self-incompatibility in *Brassica*. Science **286**: 1697–1700

Sijacic P, Wang X, Skirpan AL, Wang Y, Dowd PE, McCubbin AG, Huang S, Kao TH (2004) Identification of the pollen determinant of S-RNase-mediated self-incompatibility. Nature **429**: 302–305

Steinbachs JE, Holsinger KE (2002) S-RNase-mediated gametophytic self-incompatibility is ancestral in eudicots. Mol Biol Evol **19**: 825–829

Sudhir K, Glen S, Li M, Christina K, Koichiro T (2018) MEGA X: molecular evolutionary genetics analysis across computing platforms. Mol Biol Evol **35**: 1547–1549

Suzuki G, Kai N, Hirose T, Fukui K, Nishio T, Takayama S, Isogai A, Watanabe M, Hinata K (1999) Genomic organization of the *S* locus: identification and characterization of genes in *SLG*/*SRK* region of *S9* haplotype of *Brassica campestris* (syn. *rapa*) Genetics **153**: 391–400

Takayama S, Shiba H, Iwano M, Shimosato H, Che F, Kai N, Watanabe M, Suzuki G, Hinata K, Isogai A (2000) The pollen determinant of self-incompatibility in *Brassica campestris*. Proc Natl Acad Sci USA **97**: 1920–1925

Takayama S, Isogai A (2005) Self-incompatibility in plants. Annu Rev Plant Biol **56**: 467–489

Takasaki T, Hatakeyama K, Suzuki G, Watanabe M, Isogai A, Hinata K (2000) The *S* receptor kinase determines self-incompatibility in *Brassica* stigma. Nature **403**: 913–916

Tang C, Toomajian C, Shermanbroyles S, Plagnol V, Guo YL, Hu TT, Clark RM, Nasrallah JB, Weigel D, Nordborg M (2007) The evolution of selfing in *Arabidopsis thaliana*. Science **317**: 1070–1072

Tao R, Iezzoni AF (2010) The S-RNase-based gametophytic self-incompatibility system in *Prunus* exhibits distinct genetic and molecular features. Sci Hortic **124**: 423–433

Tomato Genome Consortium (2012) The tomato genome sequence provides insights into fleshy fruit evolution. Nature **485**: 635–641

Tsuchimatsu T, Suwabe K, Shimizuinatsugi R, Isokawa S, Pavlidis P, Städler T, Suzuki G, Takayama S, Watanabe M, Shimizu KK (2010) Evolution of self-compatibility in Arabidopsis by a mutation in the male specificity gene. Nature **464**: 1342

Ushijima K, Sassa H, Dandekar AM, Gradziel TM, Tao R, Hirano H (2003) Structural and transcriptional analysis of the self-incompatibility locus of almond: identification of a pollen expressed F-box gene with haplotype-specific polymorphism. Plant Cell **15**: 771–781

Ushijima K, Yamane H, Watari A, Kakehi E, Ikeda K, Hauck NR, Iezzoni AF, Tao R (2004) The *S* haplotype-specific F-box protein gene, *SFB*, is defective in self-compatible haplotypes of *Prunus avium* and *P. mume*. Plant J **39**: 573–586

Vaughan SP, Russell K, Sargent DJ, Tobutt KR (2006) Isolation of *S*-locus F-box alleles in *Prunus avium* and their application in a novel method to determine self-incompatibility genotype. Theor Appl Genet **112**: 856–866

Vieira J, Fonseca NA, Vieira CP (2008) An S-RNase-based gametophytic self-incompatibility system evolved only once in eudicots. J Mol Evol **67**: 179

Wheeler MJ, de Graaf BH, Hadjiosif N, Perry RM, Poulter NS, Osman K, Vatovec S, Harper A, Franklin FC, Franklin-Tong VE (2009) Identification of the pollen self-incompatibility determinant in *Papaver rhoeas*. Nature **459**: 992–995

Williams JS, Der JP, dePamphilis CW, Kao TH (2014a) Transcriptome analysis reveals the same 17 *S*-locus F-box genes in two haplotypes of the self-incompatibility locus of *Petunia inflata*. Plant Cell **26**: 2873–2888

Williams JS, Natale CA, Wang N, Li S, Brubaker TR, Sun P, Kao TH (2014b) Four previously identified *Petunia inflata S*-locus F-box genes are involved in pollen specificity in self-incompatibility. Mol Plant **7**: 567–569

Xue Y, Carpenter R, Dickinson HG, Coen ES (1996) Origin of allelic diversity in *Antirrhinum S* locus RNases. Plant Cell **8**: 805–814

Xue Y, Zhang Y, Yang Q, Li Q, Cheng Z, Dickinson HG (2009) Genetic features of a pollen-part mutation suggest an inhibitory

role for the *Antirrhinum* pollen self-incompatibility determinant. Plant Mol Biol **70**: 499–509

Ye M, Peng Z, Tang D, Yang Z, Li D, Xu Y, Zhang C, Huang S (2018) Generation of self-compatible diploid potato by knockout of *S-RNase*. Nat Plants **4**: 651–654

Zhang Y, Zhao Z, Xue Y (2009) Roles of proteolysis in plant self-incompatibility. Annu Rev Plant Biol **60**: 21–42

Zhao H, Song Y, Li J, Zhang Y, Huang H, Li Q, Zhang Y, Xue Y (2021) Primary restriction of S-RNase cytotoxicity by a stepwise ubiquitination and degradation pathway in *Petunia hybrida*. New Phytol **231**: 1249–1264

Zhou J, Wang F, Ma W, Zhang Y, Han B, Xue Y (2003) Structural and transcriptional analysis of *S-locus F-box* genes in *Antirrhinum*. Sex Plant Reprod **16**: 165–177